

DMD # 85993

1

Title Page

Original Manuscript

**A systematic *in vitro* investigation of the inhibitor preincubation effect on multiple
classes of clinically relevant transporters**

Péter Tátrai*, Patrick Schweigler, Birk Poller, Norbert Domange, Roelof de Wilde, Imad

Hanna, Zsuzsanna Gáborik, Felix Huth*

PT, RdW, ZG: Solvo Biotechnology, Budapest, Hungary

PS, BP, ND, FH: Novartis Institutes for Biomedical Research, Basel, Switzerland

IH: Novartis Institutes for Biomedical Research, East Hanover, NJ, USA

*Corresponding authors

DMD # 85993

2

Running Title Page

Running title: A systematic investigation of inhibitor preincubation

Corresponding author #1

Felix Huth, Ph.D.

Senior Investigator, PK Science – In vitro ADME

Novartis Pharma AG, Novartis Institutes of BioMedical Research

Novartis Campus St. Johann, Fabrikstr. 14, CH-4002 Basel, Switzerland

Mobile: +41 79 1579681

Fax: +41 61 6968583

felix.huth@novartis.com

Corresponding author #2

Péter Tátrai, Ph.D.

Senior Scientist, Research & Development

Solvo Biotechnology

Science Park, Building B2, 4-20 Irinyi J. Str., H-1117 Budapest, Hungary

Mobile: +36 30 386 0705

Fax: +36 62 420 617

tatrai@solvo.com

Number of text pages: 4

Number of tables: 5 Main Tables, 6 Supplementary Tables

Number of figures: 5 Main Figures, 5 Supplementary Figures

Number of references: 28

Abstract word count: 248

Introduction word count: 749

Discussion word count: 1332

List of abbreviations

BSA, bovine serum albumin

CsA, cyclosporin A

DDI, drug-drug interaction

DMEM, Dulbecco's Modified Eagle's Medium

DMSO, dimethyl sulfoxide

DS, dosing solution

EMA, European Medicines Agency

FBS, fetal bovine serum

FDA, Food and Drug Administration

HBSS, Hanks' Balanced Salt Solution

HEK, human embryonic kidney

Inh, inhibitor

MATE, multidrug and toxin extrusion

MDCK, Madin-Darby canine kidney

MDCK-LE, MDCK-low efflux

MW, molecular weight

NSB, nonspecific binding

OAT, organic anion transporter

OATP, organic anion transporting polypeptide

OCT, organic cation transporter

PMDA, Pharmaceuticals and Medical Devices Agency

PTIP, potentiation of transporter inhibition by preincubation

ROC, receiver operating characteristic

DMD # 85993

4

SFM, serum-free medium

tPSA, topological polar surface area

TTSS, time to steady state

Abstract

Preincubation of a drug transporter with its inhibitor in a cell-based assay may result in the apparent enhancement of the inhibitory potency. Currently, limited data is available on potentiation of transporter inhibition by preincubation (PTIP) for clinically relevant solute-carrier transporters other than OATP1B1 and OATP1B3. Therefore, PTIP was examined systematically using OATP1B1, OATP1B3, OAT1, OAT3, OCT1, OCT2, MATE1, and MATE2-K cell lines. IC₅₀ values of 30 inhibitors were determined with or without 3 hours of preincubation, and compounds with a PTIP $\geq 2.5x$ were further characterized by assessing the time course of transport inhibition potency and cellular concentration. For each compound, correlations were calculated between highest observed PTIP and physicochemical properties. PTIP was prevalent among OCTs and OATPs but not among OATs or MATEs, and most instances of PTIP persisted after controlling for toxicity and non-specific binding. Occasionally, preincubation in excess of 2 hours was required to attain full inhibitory potency. For 4 drugs examined, preincubation had the potential to change the *in vitro* drug-drug interaction risk prediction from 'no risk' to 'risk' based on current regulatory criteria. Molecular weight and LogD_{7.4}, as well as the ratio of passive cellular accumulation and cellular uptake rate correlated with PTIP; thus, low cellular permeation and a slow build-up of unbound intracellular inhibitor concentration may contribute to PTIP. Taken together, our data suggest that PTIP is partly determined by the physicochemical properties of the perpetrator drug, and preincubation may affect the *in vitro* predicted DDI risk for OCTs as well as OATPs.

Significance Statement

During the development of a novel pharmaceutical drug, *in vitro* studies are conducted to assess the risk of potential adverse interactions between existing medications a patient may already be taking and the novel compound. The exact way these *in vitro* assays are performed may influence the outcome of risk assessment. Here we suggest that the interaction risk may be underestimated unless specific assay protocols are modified to include an additional incubation step that allows the test drug to accumulate inside the cells, and demonstrate that adding this step is particularly important for large and hydrophobic drug molecules.

Introduction

Uptake transporters involved in drug clearance accept a broad spectrum of substrates, and their contribution to cellular uptake is especially important for low-permeability compounds. Whenever transporter-mediated uptake becomes the rate-limiting step in drug clearance, inhibition of transport may lead to clinically relevant exposure increases (Lee et al., 2017). Therefore, health authorities recommend the routine investigation of new drug candidates as transport inhibitors at various stages of clinical development (EMA, 2012; FDA, 2017; PMDA, 2018). A classic example of transporter-mediated DDI is the interference of cyclosporin A (CsA) with the OATP-mediated uptake of statins into hepatocytes (Hirano et al., 2006). By inhibiting the active cellular uptake of statins, CsA restrains their access to their hepatic target and increases exposure of peripheral tissues; thus, it simultaneously limits the efficacy of statins and increases the potential for adverse effects (Neuvonen et al., 2006).

In vitro uptake inhibition assays are highly instrumental in predicting transporter-based DDIs; however, to yield physiologically relevant predictions, these models should mimic real-life drug exposure patterns. A putative perpetrator may be administered in the clinic for prolonged periods and attain steady state concentrations in all accessible tissues before a victim drug is taken. In contrast, traditional *in vitro* assays comprise only a simultaneous incubation of the transporter with a probe substrate and the test drug. Coincubation allows only for immediate and direct interaction of the test drug with the transporter binding site and may hence underestimate DDI risk. Early evidence for this came from studies where the inhibitory effect of a single dose of CsA on the hepatic clearance of bromsulphthalein persisted for at least 3 days in rats (Shitara et al., 2009), and preincubation before coincubation of OATP1B1 with CsA, compared to coincubation only, resulted in up to 20-fold reduction in the measured IC₅₀ values (Amundsen et al., 2010; Shitara et al., 2012). Recent literature indicates that additional compounds including ritonavir, saquinavir, and anthraquinones can exert a more potent inhibition of uptake transport activity upon preincubation (Amundsen et al., 2010; Shitara et al., 2013; Ma et al., 2015; Shitara and Sugiyama, 2017).

Although this potentiation of transport inhibition by preincubation (PTIP) may at first seem to be analogous to the time-dependent inhibition of drug metabolizing enzymes, its mechanism is likely to be different. It is hypothesized that such inhibitors can interact with the transporter on both the extracellular side (*cis*) and the cytosolic side (*trans*). PTIP is thought to arise when *trans*-inhibition is more potent than *cis*-inhibition, and intracellular accumulation of the inhibitor is slow (Shitara and Sugiyama, 2017). The time requirement of maximum inhibition is compound-specific and likely correlates with the membrane permeability of the inhibitor. Another potential source of apparent PTIP in *in vitro* assays may be nonspecific binding (NSB) of the inhibitor to plasticware and/or cells during preincubation. Lipophilic compounds like saquinavir, ritonavir, or CsA may saturate available non-specific binding sites during the preincubation period, and no additional amounts of these inhibitors would be irreversibly lost during the transport step of the uptake assay.

Currently, inhibition assays for clinically relevant drug transporters other than OATPs are conducted without a preincubation step. The omission of this step can be considered a shortfall when attempting to mimic *in vivo* conditions where an inhibitor is allowed to attain steady-state tissue concentrations prior to the administration of the test substrate. Most studies concerning PTIP have focused on OATPs, prompting regulatory agencies to recommend the inclusion of a preincubation step when examining OATP transport inhibition. While sporadic studies have addressed the effect of preincubation on OATs (Ma et al., 2015) and OCTs (Arakawa et al., 2017), the lack of a systematic examination of non-OATP transporters limits the knowledge of whether such mechanisms may be of additional clinical relevance.

In this study, the preincubation effect of 30 compounds was investigated on OATP1B1, OATP1B3, OAT1, OAT3, OCT1, OCT2, as well as multidrug and toxin extrusion (MATE) 1 and MATE2-K operated in inverse (uptake) mode, and the potential impact of PTIP on transporter-based DDI risk prediction was assessed. The contribution of non-specific binding and inhibitor toxicity to PTIP was interrogated through recovery and cell viability experiments.

Correlations were sought between PTIP and physicochemical descriptors of inhibitors such as molecular weight, topological polar surface area (tPSA), cLogP, LogD_{7.4}, and passive permeability (P_{app}) to establish if any of these parameters is predictive of the PTIP behavior of a drug. Finally, cellular accumulation and inhibitory potency of selected compounds was monitored over time to see whether the extent of PTIP correlates with intracellular unbound inhibitor concentration.

Materials and Methods

Transporter cell lines

Human embryonic kidney 293 (HEK293) cell lines overexpressing the human uptake transporters OATP1B1, OATP1B3, OAT1, OAT3, OCT1, and OCT2, as well as Madin-Darby canine kidney II (MDCKII) cell lines overexpressing MATE1 and MATE2-K were created by lentiviral transduction. cDNAs were synthesized and cloned by GenScript (Piscataway, NJ), and lentiviral particles were generated in HEK293FT cells (Invitrogen/ThermoFisher, Waltham, MA). Transduced and antibiotic-selected cells were subjected to single-cell cloning, and amplified clones were functionally tested for transporter-specific uptake activity and stability of expression. Cell cultures were maintained in Dulbecco's Modified Eagle's Medium (DMEM), 4500 mg/L glucose, supplemented with GlutaMAX®, 10% v/v fetal bovine serum (FBS), and 1% v/v Penicillin-Streptomycin (all from Gibco/ThermoFisher, Waltham, MA).

Test compounds

Thirty transport inhibitors (**Table 1**) were selected to represent a broad range of molecular properties including inhibitory potencies (Drug Interaction Database, University of Washington), physicochemical characteristics, and MDCK (low efflux) permeability (for measurement and calculation methods see *Physicochemical parameters of test compounds*). Atorvastatin and pravastatin were purchased from Sequoia Research Products (Pangbourne, UK); daclatasvir, dolutegravir, isavuconazole, and ledipasvir were purchased from MedChem Express (Sollentuna, Sweden); ranitidine was purchased from abcr (Zug, Switzerland); all other inhibitors were purchased from Sigma-Aldrich (St. Louis, MI).

Physicochemical parameters of test compounds

For the determination of apparent passive permeability (P_{app}), MDCK (low efflux) cells (MDCK-LE, Sigma #8412903, selected clone with low efflux activity) were seeded on Transwell® 96-well plate inserts (Corning, Tewksbury, MA) at a density of 2.6×10^5 cells/cm² in high glucose DMEM with GlutaMAX™ containing 10% v/v FBS and 1% v/v Penicillin-Streptomycin (all from

Gibco) and grown for 4 days at 37°C in an atmosphere of 5% CO₂ and 95% relative humidity. Stock solutions of the compounds were prepared in DMSO (10 mM), and each compound was dosed in triplicate at a final concentration of 10 μM in HBSS at pH 7.4 containing 10 mM HEPES, and 0.02% w/v bovine serum albumin (BSA). Cells were incubated with the compounds for 2 hours at 37°C, and flux was measured in the apical to basolateral direction. Dosing solutions as well as the calibration solutions were centrifuged for 10 minutes at 1000× g. Drug concentrations in the donor and acceptor compartments were measured by LC-MS as described in *LC-MS sample preparation and analytics* using a 6-point calibration curve, glyburide as an analytical internal standard, and the settings listed in **Supplementary Table 1**.

LogD_{7.4} values were determined as described by Low et al. (Low et al., 2016). Topological polar surface area (tPSA) was calculated as described by Ertl et al. (Ertl et al., 2000). ClogP values were computed using CLOGP Daylight Version 4.9 (<http://www.daylight.com/dayhtml/doc/clogp/>; BioByte, Claremont, CA, USA). Cellular K_p was predicted using the method described by Yabe et al. (Yabe et al., 2011) based on logD_{7.4}:

$$\text{Eq. 1 } K_{p,pred} = \frac{1}{f_{u,cell}} = \frac{1}{10^{(-0.9161 - 0.2567 * \log D_{7.4})}}$$

Investigation of non-specific binding

A subset of test compounds was investigated for non-specific binding to plasticware. Polypropylene deep-well plates were pre-coated for 2 h at 37°C with 200 μL/well Hanks' Balanced Salt Solution (HBSS) buffer containing 20% v/v FBS and 2% w/v BSA. The coating solution was aspirated, and the plates were dried by nitrogen flow. Dosing solutions containing CsA, saquinavir, venetoclax, and ledipasvir were prepared at 0.1 μM and 1 μM in protein-free DMEM medium and dispensed into non-coated or pre-coated plates. Recovery after 0, 15, 30, 60, 120, and 180 minutes of incubation was measured by LC-MS as described below.

Uptake inhibition assays with transporter cell lines

Transporter-expressing cells and corresponding mock-transduced controls were seeded on untreated (if MDCKII-derived) or poly-D-lysine-treated (if HEK293-derived) 96-well tissue culture plates at a density of 1×10^5 cells/well. Sixteen to 20 hours after seeding, cells were rinsed twice with serum-free DMEM (SFM), then preincubated for 3 hours in the CO₂ incubator with i) SFM + dimethyl sulfoxide (DMSO) or ii) dosing solutions containing serial dilutions of the test compound in SFM. For all conditions, the final DMSO concentration was adjusted to 1% v/v.

Following preincubation, cells were rinsed twice with assay buffer, and coincubation was started with a suitable radiolabeled probe and the dilution series of the inhibitor. A reference inhibitor instead of the test inhibitor was added to control wells to determine uptake in the absence of active transport. Assay conditions and specific reagents are summarized in **Supplementary Table 2**. Uptake was terminated by rinsing twice with ice-cold assay buffer, and cells were lysed with 0.1 M NaOH. Radioactivity in cell lysates mixed with liquid scintillation cocktail (Ultima Gold XR, PerkinElmer, Waltham, MA) was measured with a MicroBeta² microplate counter (PerkinElmer).

In a first series of experiments, dosing solutions and assay reaction mixtures were kept in untreated 96-well cell culture plates (called auxiliary plates) for the duration of preincubation. In a second series, auxiliary plates were pre-coated as described in *Investigation of non-specific binding*.

Determination of IC₅₀ and PTIP values

Percent of control transport values were plotted against the logarithm of test inhibitor concentration, and IC₅₀ values were calculated using a Log(inhibitor) vs. normalized response nonlinear regression model according to **Equation 2**, where HillSlope is a dimensionless curve fitting parameter:

$$\text{Eq. 2 Transport\%} = \frac{100}{1 + 10^{(\text{Log}(IC_{50}) - \text{Log}(\text{drug concentration})) * \text{HillSlope}}}$$

PTIP was defined as the fold difference between IC_{50} values obtained without vs. with a 3-hour preincubation. PTIP values ≥ 2.5 (i.e., preincubation caused a 2.5-fold or greater decrease in IC_{50}) were considered potentially relevant, and transporter/test inhibitor pairs with PTIP ≥ 2.5 were taken forward for further investigation.

Cell viability assays and estimation of toxicity-related IC_{50} change

In single-point toxicity assays, cell viability was determined using the CellTiter-Glo® Luminescent Cell Viability Assay (Promega, Madison, WI) according to the manufacturer's instructions. Compounds that caused $\geq 10\%$ loss of viability upon 3 hours of incubation were further tested in serial dilutions, and cell viability after 3 hours of treatment was measured by resazurin assay. Briefly, following the treatment cells were rinsed and incubated for additional 1 hour with 70 μM resazurin in SFM. Resorufin formation was quantified at 544nm (Ex)/ 620 nm (Em) using a FluoStar Omega microplate reader (BMG Labtech, Ortenberg, Germany). The potential effect of toxicity on IC_{50} was estimated by multiplying %transport values measured in the no-preincubation setting with %viability at each compound concentration. An inhibition curve was fitted on the viability-modulated %transport values according to **Equation 2**, IC_{50} was computed, and the fold change in IC_{50} potentially caused by toxicity was calculated.

DDI risk prediction based on in vitro results

Guidelines issued by the U.S. Food and Drug Administration (FDA), the European Medicines Agency (EMA), and the Japanese Pharmaceuticals and Medical Devices Agency (PMDA) recommend the *in vitro* determination of IC_{50} or K_i for each novel drug candidate, and define formulas for the estimation of DDI risk based on the relationship of IC_{50} or K_i to the unbound maximum plasma concentration in the systemic circulation or at the hepatic inlet (**Supplementary Table 3**). Due to the uncertainties inherent to the calculation of maximum hepatic inlet concentration we have chosen to estimate DDI risk for each transporter (including hepatic transporters) based on $C_{\text{max,u,ss}} / IC_{50}$, where $C_{\text{max,u,ss}}$ was calculated as $C_{\text{max,ss}}$, the maximum plasma concentration at steady state, multiplied by f_u , the unbound fraction. $C_{\text{max,ss}}$

and f_u were taken from the literature or the respective product labels (for references see **Table 4**), and f_u values were replaced with 0.01 whenever the experimentally determined value was lower than 0.01.

Time course of PTIP

Transporter-expressing cells were preincubated for 15, 30, 60, 90, 120, and 180 min with test inhibitors previously shown to exhibit $PTIP \geq 2.5$ upon 3 hours of preincubation. For each group, the total preincubation time of 180 min was split into a DMSO-only and an inhibitor interval (e.g., the 30-min group was first incubated with DMSO for 150 min and then with inhibitor for 30 min). The control group was preincubated for 180 min with 1% v/v DMSO. After 180 min, an uptake assay was performed as described in *Uptake inhibition assays*.

Time course of cellular inhibitor concentration

Transporter-expressing cells were seeded at a density of 5×10^5 cells/well in poly-D-lysine-coated 24-well plates and grown for 16-18 hours. Before the experiment, a dosing solution (DS) containing the test compound was prepared in SFM, and the reference inhibitor of the transporter was added to an aliquot of the dosing solution (DS+Inh). An auxiliary 24-well plate used to contain DS and DS+Inh was pre-coated with 20% FBS / 2% BSA to decrease non-specific plastic binding of the test compound.

Treatment groups were incubated with DS for 1, 3, 5, 15, 30, 60, 90, 120, and 180 min, or with DS+Inh for 60 min and 180 min. The control group was incubated with SFM + DMSO for 180 min. Treatment groups incubated with DS+Inh, where the respective transporter was blocked, were included to assess the relative contribution of transporter-mediated uptake. For each group, the total preincubation time of 180 min was split into a DMSO-only and an inhibitor interval. Dosing solutions DS and DS+Inh were sampled at each dosing time point. At the endpoint (180 min), all supernatants were sampled, plates were placed on ice, cells were washed twice with ice-cold HBSS and extracted for 5 min with a 2:1 mixture of acetonitrile and

deionized water. Collected samples of dosing solutions and supernatants were mixed 1:1 with acetonitrile.

LC-MS sample preparation and analytics

Cell extracts as well as dosing solution and supernatant samples were diluted as necessary and injected to LC-MS after addition of 0.5 μM glyburide as internal standard. The compounds were separated on a Phenomenex Synergi RP Polar column (2.5 μM , 30 \times 2.1 mm; Phenomenex, Aschaffenburg, Germany) using water and acetonitrile including 0.1% formic acid (v/v) as mobile phases in gradient modes. The HPLC system was coupled to a QTRAP5500 mass spectrometer (AB Sciex LLC, Framingham, MA) using an electrospray interface. The MS was operated in multiple reaction monitoring mode using the transitions shown in **Supplementary Table 1**. Data analysis was done with DiscoveryQuant and MultiQuant software (AB Sciex LLC).

Calculation of cellular uptake parameters

The cellular uptake was expressed as a clearance (PS_{inf} ; $\mu\text{L}/\text{min}/10^6$ cells) calculated from the slope of the initial linear uptake phase normalized for the cell number (V_{inf} ; $\text{pmol}/\text{min}/10^6$ cells) and the applied concentration at time zero (C_0 ; μM):

$$\text{Eq. 3 } PS_{inf} = \frac{V_{inf}}{C_0}$$

K_p describes the steady-state distribution of a compound between the cell and the medium and is calculated as the ratio of cellular and medium concentration at steady state ($C_{cell,ss}$ / $C_{medium,ss}$). When excluding active transport processes by the addition of an appropriate transporter inhibitor and assuming an unbound fraction (f_u) of 1 in the protein-free medium, the unbound cellular fraction ($f_{u,cell}$) can be derived as the reciprocal of K_p . $C_{cell,ss}$ was calculated based on the total cell number (5×10^5 /well) and a cell volume of 0.8 $\mu\text{L}/10^6$ cells.

$$\text{Eq. 4 } K_p = \frac{C_{cell,ss}}{C_{medium,ss}} = \frac{1}{f_{u,cell}}$$

$K_{p,uu}$ is defined as the ratio of the unbound cellular concentration and the unbound medium concentration at steady state. $K_{p,uu}$ can be calculated as the ratio of K_p values determined in the absence and presence of a reference inhibitor, assuming active transport was completely inhibited in the latter condition.

$$\mathbf{Eq. 5} \quad K_{p,uu} = \frac{K_p(-\text{inhibitor})}{K_p(+\text{inhibitor})}$$

Statistical analysis

GraphPad Prism 7.03 (GraphPad Software, La Jolla, CA) was used to perform nonlinear regression, Receiver Operating Characteristic (ROC) analysis, as well as to calculate Spearman's rank correlations. PTIP-positive or PTIP-negative status was assigned to each inhibitor depending on whether it displayed $\text{PTIP} \geq 2.5$ in any assay, and ROC analysis was used to find cut-off values of physicochemical parameters that predict PTIP status with high sensitivity and specificity. Fisher's exact test of contingency tables was done using VassarStats (<http://vassarstats.net/>). P values < 0.05 were considered as significant.

Results

Occurrence of PTIP among inhibitors of OATPs, OATs, OCTs, and MATEs

Uptake inhibition assays were performed using HEK-OATP1B1, HEK-OATP1B3, HEK-OAT1, HEK-OAT3, HEK-OCT1, HEK-OCT2, MDCKII-MATE1, and MDCKII-MATE2-K cell lines with or without a 3-h preincubation step. Since the phenomenon of PTIP has been most extensively studied on OATPs, only 6 compounds including the model time-dependent inhibitor CsA were examined in this set of studies. PTIP mediated by OATs, OCTs, and MATEs was examined with 10, 14, and 8 inhibitors, respectively. Seventy-six transporter/inhibitor combinations were analyzed in total. Based on the analysis of all PTIP values including expected positives and negatives, the threshold for positive PTIP was set to 2.5-fold difference between IC₅₀ values obtained without vs. with preincubation.

Initially, dosing solutions and assay reaction mixtures were prepared in untreated 96-well cell culture plates (called auxiliary plates) and kept there for the duration of preincubation. Subsequently, assays with a positive PTIP result were repeated (N=2) using auxiliary plates pre-coated with 20% v/v FBS and 2% w/v BSA. This surface treatment was shown to effectively reduce time-dependent nonspecific binding (NSB) of four notoriously plastic-adherent compounds, saquinavir, CsA, venetoclax, and ledipasvir (**Supplementary Fig.1**).

PTIP values from the initial series of experiments performed in uncoated plates ('NSB block -') as well as from confirmatory experiments using pre-coated plates ('NSB block +') are shown in **Table 2**. All corresponding IC₅₀ values are listed in **Supplementary Table 4**. In the 'NSB block -' experiments, 3 out of 6 OATP inhibitors, 1 out of 10 OAT inhibitors, 9 out of 14 OCT inhibitors, and 2 out of 8 MATE inhibitors were found to exhibit PTIP on at least one member of the respective transporter family. The most pronounced preincubation effect was observed with ledipasvir on HEK-OCT1 cells, and venetoclax on HEK-OATP1B1 cells (**Fig.1, A and D**). Ledipasvir had a similar, albeit smaller, effect on OCT2 transport activity when this transporter was expressed in HEK293 or MDCKII cells, suggesting that the inhibition specifically targets

OCT activity and is not an artifact due the use of a particular host cell line (**Fig. 1, B-C**). Some inhibitors showed PTIP on multiple transporter families (saquinavir on OATP1Bs and OCT1; isavuconazole and vandetanib on OCTs and MATE2-K). Taking these overlaps into account, 12 out of 30 (40%) inhibitors showed PTIP on at least one transporter.

Experiments repeated with pre-coated auxiliary plates verified the PTIP-positive status of 10 inhibitors. Initial positive results were not confirmed for benzbromarone and cetirizine. Additionally, isavuconazole turned out to be PTIP-negative on MATE2-K but remained PTIP-positive on both OCTs. Venetoclax/OATP1B1 and ledipasvir/OCT1 experiments were also repeated with 1% w/v BSA present throughout all steps including washes, preincubation, and coincubation. Although the addition of BSA changed the apparent IC₅₀ values and reduced the difference between the no-preincubation and preincubation conditions, PTIP with BSA remained 25-fold or higher for both compounds (**Supplementary Fig.2**).

The effect of PTIP-positive inhibitors on cell viability

A 3-hour treatment with a single high dose of confirmed PTIP-positive inhibitors has indicated no toxicity (cell viability $\geq 90\%$) for CsA, daclatasvir, dolutegravir, irinotecan, or ledipasvir (**Supplementary Table 5**). Isavuconazole at 300 μM was selectively toxic to HEK-OCT2 cells, while saquinavir at 100 μM impaired the viability of HEK-OATP1B1 and HEK-OATP1B3 but not of HEK-OCT1. Venetoclax at 100 μM was moderately toxic to both HEK-OATP1B1 and HEK-OATP1B3, and verapamil at 100 μM mildly affected HEK-OCT1 viability. Vandetanib had the most severe effect on all treated cell lines as it caused complete cell detachment when applied at 300 μM .

Compounds that reduced cell viability by $\geq 10\%$ at high doses were further tested in serial dilutions using the resazurin viability assay. Modelled inhibition curves reflecting the toxic effect of preincubation superimposed on transporter inhibition without preincubation were overlaid on the actual inhibition curves measured without and with preincubation (**Supplementary Fig.3**), and corresponding IC₅₀ values were calculated. **Table 3** displays

preincubation-related IC_{50} changes with and without correction for reduced viability. For inhibitors with no apparent toxicity, the latter value was postulated to be 1.0. Although the toxic effect of isavuconazole, vandetanib, and venetoclax was sufficient to alter IC_{50} measurements (toxicity caused an estimated 1.4-, 1.5-, and 4.8-fold decrease in IC_{50} , respectively), all 10 inhibitors remained PTIP-positive after this correction.

The effect of assay duration on the magnitude of PTIP

For PTIP-positive inhibitors (excluding venetoclax and ledipasvir where no definite values for PTIP could be determined), the magnitude of PTIP generally decreased with longer assay incubation times. PTIP was, on average, 13.0 ± 12.7 -fold in 1-min assays (OCT2, N=5), 4.28 ± 1.70 -fold in 3-min assays (OATP1B1/3, N=4), 3.98 ± 1.30 -fold in 5-min assays (OCT1, N=6), and 1.93 ± 0.74 -fold in 15-min assays (MATE1/2-K, N=4). In particular, daclatasvir PTIP was 34.2 (OCT2) versus 5.65 (OCT1), isavuconazole PTIP was 13.2 (OCT2) versus 3.15 (OCT1) versus 1.53/1.59 (MATE1/2-K), and vandetanib PTIP was 4.19 (OCT2) versus 2.69 (OCT1) versus 1.81/3.00 (MATE1/2-K) (**Fig.2**). In line with this notion, when OATP1B1/CsA inhibition assay was performed with no preincubation but for multiple assay durations (1, 2, 5, 10, and 15 min), IC_{50} fell 7.91-fold from 0.878 μ M at 1 min to 0.111 μ M at 15 min (**Supplementary Fig.4**), suggesting that, depending on the kinetics of inhibition, an extended coincubation may leave less or no room for preincubation to make a difference.

The relevance of PTIP to in vitro DDI risk assessment

Using IC_{50} data of confirmed PTIP-positive clinical compounds from the second set of experiments ('NSB block +') we projected the impact of preincubation on the outcome of DDI risk prediction. $C_{max,u,ss}/IC_{50}$ values were calculated from IC_{50} values without vs. with preincubation and compared against cut-off values recommended by FDA, PMDA, and EMA (see **Supplementary Table 3**). For each drug, the outcome of *in vitro* DDI risk prediction was 'risk' if $C_{max,u,ss}/IC_{50}$ exceeded the respective cut-off value in any of the assays performed with that compound, and 'no risk' otherwise. As shown in **Table 4**, preincubation did not affect the

outcome for CsA, isavuconazole, ledipasvir, or venetoclax. For daclatasvir, 'risk' was predicted with both no-preincubation and preincubation conditions according to EMA, but preincubation changed the outcome to 'risk' when the higher FDA/PMDA cut-off was applied. For dolutegravir and saquinavir, $C_{\max,u,ss}/IC_{50}$ with preincubation exceeded the EMA cut-off but not the FDA/PMDA cut-off; thus, the outcome changed to 'risk' according to the EMA criteria only. Finally, in the case of irinotecan and vandetanib if only the recommended OCT2 assay was considered, preincubation changed the EMA outcome from 'no risk' to 'risk', while the OCT1 and/or MATE assays (which are optional to conduct as per EMA guidelines) predicted 'risk' even without preincubation. Hence, whether preincubation changed the EMA outcome for irinotecan and vandetanib depended on the panel of assays considered.

Correlation of PTIP with physicochemical descriptors of the test inhibitors

Table 1 lists the physicochemical parameters and highest observed PTIP values (except for pravastatin for which no IC_{50} value could be determined) for all test compounds. Molecular weight (MW), topological polar surface area (tPSA), cLogP, $\text{LogD}_{7.4}$, MDCK-LE P_{app} , K_p predicted from $\text{LogD}_{7.4}$ ($K_{p, \text{pred}}$), as well as the ratio $K_{p, \text{pred}} / \text{MDCK-LE } P_{\text{app}}$ were plotted against PTIP (**Fig.3**). Spearman's rank correlations were calculated between PTIP and each physicochemical descriptor.

Of the 7 parameters considered, MW, $\text{LogD}_{7.4}$, $K_{p, \text{pred}}$, and $K_{p, \text{pred}} / \text{MDCK-LE } P_{\text{app}}$ showed significant correlation with PTIP (Spearman's rho $r_{\text{Sp}}=0.68, 0.67, 0.67,$ and $0.58,$ respectively). On the other hand, tPSA, cLogP, and MDCK-LE P_{app} alone showed only weak or no correlation with PTIP. The descriptors were also found to be inter-correlated (for the correlation matrix see **Supplementary Table 6**; note that $K_{p, \text{pred}}$ was calculated from $\text{LogD}_{7.4}$, hence the r_{Sp} of 1.0).

To assess the predictive value of MW, $\text{LogD}_{7.4}$, $K_{p, \text{pred}}$, and $K_{p, \text{pred}} / \text{MDCK-LE } P_{\text{app}}$ with regard to PTIP status, ROC analysis was performed to find cut-off values with best sensitivity and specificity. MW > 437 g/mol was the best single predictor of PTIP+ status (sensitivity: 0.90 /

specificity: 0.89, Fisher's exact test: $P=0.00007$), followed by $\text{LogD}_{7.4} > 1.85$ or, equivalently, $K_{p, \text{pred}} > 24.85$ (sensitivity: 0.90 / specificity: 0.83, $P=0.00027$, for both). $K_{p, \text{pred}} / \text{MDCK-LE } P_{\text{app}}$ values greater than 9 predicted positive PTIP with a sensitivity of 0.70 and a specificity of 0.89 ($P=0.0028$).

Cellular uptake of inhibitors and PTIP: time-course experiments

Cellular uptake over time was investigated for the PTIP-positive inhibitors ledipasvir, venetoclax, CsA, and saquinavir, the PTIP-negative inhibitors valsartan and trimethoprim, as well as for benzbromarone that was PTIP-positive when using untreated auxiliary plates but turned negative upon plate precoating. Compounds were applied at concentrations close to the IC_{50} value with preincubation. Cellular uptake parameters are shown in **Table 5**; for comparability across PTIP-positive and PTIP-negative compounds, 'NSB block -' PTIP values were used in calculations.

Cell concentration time profiles are shown in **Fig.4** together with the degree of transport inhibition that was determined in independent experiments. Cellular concentrations did not reach steady-state over the 180-min interval for ledipasvir and venetoclax, and for both compounds the degree of transport inhibition reached its maximum after a 120-min preincubation. Time to cellular steady-state concentration was approx. 120 min for CsA and 60 min for saquinavir. With CsA, transport inhibition peaked after 90-120 min of preincubation; similarly, saquinavir reached maximum inhibition at 120 min. Cellular concentrations of benzbromarone reached steady-state after 60 min in OAT3 and 15 min in OAT1, but the degree of OAT3 inhibition was hardly affected by the duration of preincubation, which may explain the lack of observed PTIP. The PTIP-negative inhibitors valsartan and trimethoprim were identified as substrates of their respective transporters by $K_{p, \text{uu}}$ values >1 , and their cellular concentrations equilibrated rapidly with the medium (3 min and 1 min to steady-state, respectively).

When looking for associations between 3-hour PTIP and cellular uptake parameters (**Fig.5**), strong positive rank correlation was found between PTIP and time to steady-state (TTSS) ($r_{sp}=0.99$, $P=0.0002$), as well as between PTIP and the ratio composed of passive cellular accumulation over initial influx, $K_{p,passive}/PS_{inf}$ ($r_{sp}=0.98$, $P=0.0004$). Moreover, $K_{p,passive}/PS_{inf}$ and TTSS were positively intercorrelated ($r_{sp}=0.96$, $P=0.0006$), whereas the negative correlation between PS_{inf} alone and TTSS fell short of being significant ($r_{sp}=-0.70$, $P=0.06$).

Discussion

The recent FDA guidance recommends a 30-minute preincubation when investigating the inhibitory potential of a test article against OATP1B1 and OATP1B3 (FDA, 2017). Little is known about the effect of preincubation on other transporters, or the molecular properties that predispose some compounds to PTIP.

Here we investigated the preincubation effect of 30 miscellaneous compounds on OATP1B1, OATP1B3, OAT1, OAT3, OCT1 OCT2, MATE1 and MATE2-K. A prolonged preincubation of 3 hours was chosen to allow for the equilibration of compounds with low permeability between the extracellular and intracellular compartments. Preincubation caused a shift towards lower IC₅₀ values for the majority of compounds, and for 10 inhibitors the apparent potentiation was ≥2.5-fold (**Table 2**). A PTIP effect ≥2.5-fold was seen for half of OATP1B inhibitors and also more than half of OCT inhibitors, but not confirmed for OATs or MATEs.

A possible explanation for the higher frequency of PTIP among OCTs versus MATEs is the longer incubation time in MATE assays. PTIP ≥2.5-fold was mostly observed for OATP1Bs and OCTs with assay times between 1 and 5 min, while in MATE assays a 15-minute coincubation may have allowed inhibitors to equilibrate between the medium and intracellular space. The following findings support the notion that the preincubation effect is more pronounced when the subsequent coincubation is brief: i) assays with shorter incubation time were generally associated with higher PTIP values, ii) the PTIP effect of daclatasvir and isavuconazole was inversely related to assay duration (**Fig.2**), and iii) prolonged coincubation markedly decreased IC₅₀ of CsA on OATP1B1 (**Supplementary Fig.4**).

This argument, however, fails to explain why no PTIP was observed for OAT assays with short incubation times (1 or 2 min). While most investigated OAT inhibitors either had a comparatively high passive permeability P_{app} (> 3×10⁻⁶ cm/s) or were reported to be OAT substrates, bumetanide was also PTIP-negative despite a low MDCK-LE P_{app} (1.13×10⁻⁶ cm/s). The possible OAT-mediated bumetanide transport was not investigated in this study.

In general, we cannot exclude that other compounds not tested herein or the same compounds under different conditions may exhibit PTIP on OATs or MATEs. Literature data on OAT-based preincubation effect exist (Ma et al., 2015), and the PTIP liability of MATEs cannot be dismissed solely based on our results. Ultimately, it can also be speculated that some transporter families may be more prone to PTIP than others due to inherent differences in protein structure or mechanism of transport.

Upon confirmation of the novel PTIP-positive inhibitors towards OATP1Bs and OCTs, additional investigations were done to verify the mechanism behind this phenomenon. Some PTIP-positive compounds were known to exhibit strong NSB, and the preincubation effect could have been mimicked by time-dependent adsorption of test compounds to the transport apparatus. While this issue was not addressed in our first series of experiments, on repeating the PTIP-positive assays we utilized precoated plates in an attempt to minimize NSB. Reassuringly, the preincubation effect was confirmed in 19 out of 23 instances. Additionally, we re-examined the most distinct cases of PTIP (venetoclax/OATP1B1 and ledipasvir/OCT1) in the presence of 1% w/v BSA that was expected to limit binding the nonspecific binding (**Supplementary Fig.2**). As PTIP was not eliminated by the addition of BSA, a major role of NSB in the preincubation effect seemed unlikely.

Cytotoxicity of the test compounds was considered as another potential confounding factor. While toxicity of an inhibitor is barely of concern in a conventional assay containing a short coincubation only, a 3-hour preincubation with the same compound may severely compromise cell viability and/or attachment. Unless substrate uptake is normalized for total cellular protein content, cell loss or impaired viability may be mistaken for transport inhibition. Five out of 10 PTIP-positive compounds caused marked cell death; however, toxic concentration ranges were typically 10- to 100-fold higher than the respective IC_{50} values. Thus, except for a single case (venetoclax on HEK-OATP1B3), toxicity had minor or no contribution to the preincubation effect.

Taken together, these experiments highlighted OCTs as a new family of uptake transporters sensitive to preincubation and confirmed PTIP as a true effect not caused by NSB and/or toxicity. Experiments proving ledipasvir PTIP in MDCKII-OCT2 cells (**Fig.1**) raised confidence that our findings were not exclusive to HEK293 cells.

Importantly, by calculating $C_{\max,u,ss}/IC_{50}$ values without and with preincubation we have shown that preincubation may alter the outcome of *in vitro* DDI risk assessment. In our experiments, preincubation changed the DDI prediction from 'no risk' to 'risk' for dolutegravir, irinotecan, saquinavir, and vandetanib according to the EMA guidelines. Clinical data have confirmed vandetanib and dolutegravir as perpetrators of transporter-based DDI (Reese et al., 2013; Johansson et al., 2014). Of note, preincubation did not change the predicted DDI risk of ledipasvir and venetoclax despite their robust PTIP effects. This is because both drugs have extremely low measured plasma f_u values (<0.002 for ledipasvir, 0.000013 for venetoclax) (FDA, 2014; Emami Riedmaier et al., 2018). Even if f_u is set to 0.01 as a "worst-case" assessment, the $C_{\max,u,ss}/IC_{50}$ ratio remains below the cut-off.

To elucidate the possible mechanism of the preincubation effect we measured the time profiles of cellular concentration and transport inhibition. For ledipasvir, venetoclax, and CsA, cellular concentration and inhibitory potency followed remarkably similar time courses (**Fig.4**). Whereas the measured PS_{inf} values did not correlate significantly with TTSS, the correlation could be greatly improved by dividing PS_{inf} by $K_{p,passive}$ (**Fig.5**). The latter describes the steady-state passive distribution of a compound between the cells and the medium, and in a protein-free medium high $K_{p,passive}$ values indicate substantial cellular binding. Low passive permeation combined with high cellular binding results in a slow build-up of intracellular unbound drug concentration. Our data support that intracellular unbound perpetrator concentration is a major determinant of inhibitory potency and, consequently, the magnitude of PTIP depends on the equilibration time.

To explore whether PTIP can be predicted from *a priori* physicochemical parameters, we correlated PTIP with MDCK-LE permeability and molecular properties. Unlike tPSA, cLogP,

or MDCK-LE P_{app} , physicochemical descriptors including MW, $\text{LogD}_{7.4}$ and the $\text{LogD}_{7.4}$ -derived $K_{p,pred}$, as well as $K_{p,pred} / \text{MDCK-LE } P_{app}$ correlated with the preincubation effect (**Fig.3**). High (> ca. 440 Da) MW was the most reliable predictor of PTIP-positive behavior. Although the data plots were suggestive of a linear relationship between $\text{Log}(\text{PTIP})$ and $K_{p,pred}$, as well as $\text{Log}(\text{PTIP})$ and $K_{p,pred} / \text{MDCK-LE } P_{app}$, these data series were skewed by the few high-PTIP inhibitors such as venetoclax and ledipasvir. Therefore, an attempt to quantitatively predict PTIP based on these two parameters would be too ambitious until more data are collected.

It remains to be seen whether *in vitro* assays with preincubation produce more physiologically relevant data for physiology-based pharmacokinetic (PBPK) models. Underestimated inhibitory potency is among the many reasons why *in vitro* data-fed PBPK models perform poorly at predicting transporter-based DDI (Jamei et al., 2014; Pan et al., 2016). Preincubation improved the predictivity of a PBPK model describing the interaction of CsA with OATP1B1 (Shitara and Sugiyama, 2017). It will also need to be tested if preincubation can help decrease high inter-laboratory variation in transporter inhibition data. Reported IC_{50} or K_i values of OATP1B1 inhibitors sometimes vary across several orders of magnitude (Vaidyanathan et al., 2016). Here we also showed that without preincubation, extending assay duration from 1 to 15 min caused an almost 8-fold decrease in IC_{50} (**Supplementary Fig.4**).

In summary, we demonstrate that PTIP *in vitro* affects transport activity of OCTs as well as of OATP1Bs. Our data demonstrate that the inclusion of appropriate control experiments is crucial to correctly conclude whether true PTIP is observed. Most notably, control experiments to exclude effects of nonspecific binding and cellular toxicity as confounding factors should be performed. Since PTIP results in reduced IC_{50} values, the number of positive *in vitro* DDI risk predictions is generally expected to increase, unless $1/\text{IC}_{50}$ cut-off values in guidelines are adjusted accordingly. The propensity of an inhibitor for PTIP depends on molecular properties such as high molecular weight and hydrophobicity, and a slow build-up of the unbound intracellular perpetrator drug concentration is a prerequisite for the preincubation effect.

Acknowledgments

The authors would like to acknowledge John P. Keogh (JPK Consulting, Hitchin, United Kingdom) for his invaluable help with the initiation of the project and suggestions on the study design, and Stephane Rodde (Novartis Pharma AG) for measuring LogD_{7.4} values.

Authorship Contributions

Participated in research design: Tátrai, Schweigler, Poller, Domange, Hanna, de Wilde, Gáborik, Huth

Conducted experiments: Tátrai, Domange

Contributed new reagents or analytic tools: Poller, Domange, Huth

Performed data analysis: Tátrai, Schweigler, Poller, Domange, Gáborik, Huth

Wrote or contributed to the writing of the manuscript: Tátrai, Schweigler, Poller, Domange, Hanna, de Wilde, Gáborik, Huth

References

- Amundsen R, Christensen H, Zabihiyan B, and Asberg A (2010) Cyclosporine A, but not tacrolimus, shows relevant inhibition of organic anion-transporting protein 1B1-mediated transport of atorvastatin. *Drug metabolism and disposition: the biological fate of chemicals* **38**:1499-1504.
- Arakawa H, Omote S, and Tamai I (2017) Inhibitory Effect of Crizotinib on Creatinine Uptake by Renal Secretory Transporter OCT2. *Journal of pharmaceutical sciences* **106**:2899-2903.
- EMA (2012) Guideline on the investigation of drug interactions, EMA.
- Emami Riedmaier A, Lindley DJ, Hall JA, Castleberry S, Slade RT, Stuart P, Carr RA, Borchardt TB, Bow DAJ, and Nijssen M (2018) Mechanistic Physiologically Based Pharmacokinetic Modeling of the Dissolution and Food Effect of a Biopharmaceutics Classification System IV Compound-The Venetoclax Story. *Journal of pharmaceutical sciences* **107**:495-502.
- Ertl P, Rohde B, and Selzer P (2000) Fast calculation of molecular polar surface area as a sum of fragment-based contributions and its application to the prediction of drug transport properties. *Journal of medicinal chemistry* **43**:3714-3717.
- FDA (2013) TIVICAY (dolutegravir),
https://www.accessdata.fda.gov/drugsatfda_docs/label/2013/204790lbl.pdf.
- FDA (2014) HARVONI TM (ledipasvir and sofosbuvir),
https://www.accessdata.fda.gov/drugsatfda_docs/label/2014/205834s000lbl.pdf.
- FDA (2015a) CRESEMBA® (isavuconazonium sulfate)
https://www.accessdata.fda.gov/drugsatfda_docs/label/2015/207500Orig1s000lbl.pdf
- FDA (2015b) DAKLINZA (daclatasvir),
https://www.accessdata.fda.gov/drugsatfda_docs/label/2015/206843Orig1s000lbl.pdf

- FDA (2017) In Vitro Metabolism and Transporter Mediated Drug-Drug Interaction Studies Guidance for Industry, FDA.
- Goodman L, Hardman J, Limbird L, and Gilman A (2001) *Goodman & Gilman's the pharmacological basis of therapeutics. 10th ed.* . New York : McGraw-Hill, Medical Pub. Division, c2001.
- Hirano M, Maeda K, Shitara Y, and Sugiyama Y (2006) Drug-drug interaction between pitavastatin and various drugs via OATP1B1. *Drug metabolism and disposition: the biological fate of chemicals* **34**:1229-1236.
- Jamei M, Bajot F, Neuhoff S, Barter Z, Yang J, Rostami-Hodjegan A, and Rowland-Yeo K (2014) A mechanistic framework for in vitro-in vivo extrapolation of liver membrane transporters: prediction of drug-drug interaction between rosuvastatin and cyclosporine. *Clinical pharmacokinetics* **53**:73-87.
- Johansson S, Read J, Oliver S, Steinberg M, Li Y, Lisbon E, Mathews D, Leese PT, and Martin P (2014) Pharmacokinetic evaluations of the co-administrations of vandetanib and metformin, digoxin, midazolam, omeprazole or ranitidine. *Clinical pharmacokinetics* **53**:837-847.
- Lee SC, Arya V, Yang X, Volpe DA, and Zhang L (2017) Evaluation of transporters in drug development: Current status and contemporary issues. *Advanced drug delivery reviews* **116**:100-118.
- Low YW, Blasco F, and Vachaspati P (2016) Optimised method to estimate octanol water distribution coefficient (logD) in a high throughput format. *European journal of pharmaceutical sciences : official journal of the European Federation for Pharmaceutical Sciences* **92**:110-116.
- Ma L, Qin Y, Shen Z, Hu H, Zhou H, Yu L, Jiang H, and Zeng S (2015) Time-Dependent Inhibition of hOAT1 and hOAT3 by Anthraquinones. *Biological & pharmaceutical bulletin* **38**:992-995.

- Neuvonen PJ, Niemi M, and Backman JT (2006) Drug interactions with lipid-lowering drugs: mechanisms and clinical relevance. *Clinical pharmacology and therapeutics* **80**:565-581.
- Pan Y, Hsu V, Grimstein M, Zhang L, Arya V, Sinha V, Grillo JA, and Zhao P (2016) The Application of Physiologically Based Pharmacokinetic Modeling to Predict the Role of Drug Transporters: Scientific and Regulatory Perspectives. *Journal of clinical pharmacology* **56 Suppl 7**:S122-131.
- PMDA (2018) Regarding medicinal herbs examiner 0723 No. 4 "About " drug interaction guidelines for drug development and proper information provision PMPA.
- Reese MJ, Savina PM, Generaux GT, Tracey H, Humphreys JE, Kanaoka E, Webster LO, Harmon KA, Clarke JD, and Polli JW (2013) In vitro investigations into the roles of drug transporters and metabolizing enzymes in the disposition and drug interactions of dolutegravir, a HIV integrase inhibitor. *Drug metabolism and disposition: the biological fate of chemicals* **41**:353-361.
- Shitara Y, Nagamatsu Y, Wada S, Sugiyama Y, and Horie T (2009) Long-lasting inhibition of the transporter-mediated hepatic uptake of sulfobromophthalein by cyclosporin a in rats. *Drug metabolism and disposition: the biological fate of chemicals* **37**:1172-1178.
- Shitara Y and Sugiyama Y (2017) Preincubation-dependent and long-lasting inhibition of organic anion transporting polypeptide (OATP) and its impact on drug-drug interactions. *Pharmacology & therapeutics* **177**:67-80.
- Shitara Y, Takeuchi K, and Horie T (2013) Long-lasting inhibitory effects of saquinavir and ritonavir on OATP1B1-mediated uptake. *Journal of pharmaceutical sciences* **102**:3427-3435.
- Shitara Y, Takeuchi K, Nagamatsu Y, Wada S, Sugiyama Y, and Horie T (2012) Long-lasting inhibitory effects of cyclosporin A, but not tacrolimus, on OATP1B1- and OATP1B3-mediated uptake. *Drug metabolism and pharmacokinetics* **27**:368-378.
- Tamura T, Minami H, Yamada Y, Yamamoto N, Shimoyama T, Murakami H, Horiike A, Fujisaka Y, Shinkai T, Tahara M, Kawada K, Ebi H, Sasaki Y, Jiang H, and Saijo N

(2006) A phase I dose-escalation study of ZD6474 in Japanese patients with solid, malignant tumors. *Journal of thoracic oncology : official publication of the International Association for the Study of Lung Cancer* **1**:1002-1009.

Vaidyanathan J, Yoshida K, Arya V, and Zhang L (2016) Comparing Various In Vitro Prediction Criteria to Assess the Potential of a New Molecular Entity to Inhibit Organic Anion Transporting Polypeptide 1B1. *Journal of clinical pharmacology* **56** **Suppl 7**:S59-72.

Yabe Y, Galetin A, and Houston JB (2011) Kinetic characterization of rat hepatic uptake of 16 actively transported drugs. *Drug metabolism and disposition: the biological fate of chemicals* **39**:1808-1814.

DMD # 85993

33

Footnotes

None

Legends for Figures

Figure 1. The preincubation effect of ledipasvir and venetoclax on OCTs and OATP1B1, respectively. IC₅₀ values without preincubation could not be determined due to weak inhibition. Each measurement point represents N=3 replicates from a single experiment.

Figure 2. PTIP and assay duration. On average, higher PTIP values were observed in shorter assays, and inhibitors applied in multiple assays (e.g. daclatasvir, isavuconazole) tended to display higher PTIP in assays with shorter incubation time.

Figure 3. Correlation of PTIP with physicochemical descriptors. PTIP showed significant nonparametric (Spearman's) correlation with molecular weight (**A**), LogD_{7.4} (**B**), K_{p,pred} (**C**), and K_{p,pred}/MDCD-LE P_{app} (**D**), but not with tPSA (**E**), cLogP (**F**), or MDCK-LE P_{app} alone (**G**). Black dotted vertical lines indicate the PTIP threshold of 2.5; red dotted horizontal lines indicate the cut-off values determined by ROC analysis and used for the calculation of specificity/sensitivity. Instead of the indeterminate PTIP ranges of ledipasvir and venetoclax (>255 and >258) the respective minima were used (=255 and =258; red symbols).

Figure 4. Cellular concentration and inhibition potency of selected inhibitors over time. Cellular concentration (green) was measured at multiple time points between 1-180 min; also, in the case of PTIP-positive inhibitors, inhibition potency (red) was determined at multiple preincubation durations ranging between 15-180 min. Dotted vertical lines indicate the time required to reach steady-state cellular concentration. Each point represents the mean ± SD of N=3 replicates. For benzbromarone (OAT1), valsartan, and trimethoprim, no potency time profiles were recorded as no PTIP effect was observed, which is in line with steady state concentrations being reached within a few minutes.

Figure 5. Associations between PTIP and cellular uptake parameters. Correlations were calculated from data shown in **Table 5**. Positive association was found between PTIP and time to steady state (TTSS), as well as PTIP and K_{p,passive}/PS_{inf} (**A-B**). The latter parameter was also positively correlated with TTSS (**C**), whereas no significant correlation was found

between PS_{inf} and TTSS (**D**). Instead of the indeterminate PTIP and/or TTSS ranges of ledipasvir and venetoclax the respective minimum values are shown (red symbols). NS, not significant.

Tables

Table 1. Physicochemical parameters vs. highest confirmed PTIP values of all test compounds used. Molecular properties were measured (LogD_{7.4}, MDCK-LE P_{app}), or calculated (tPSA, cLogP, K_{p,pred}) as described in *Materials and methods*. Highest PTIP values for each inhibitor are extracted from Table 2; where available, PTIP determined under 'NSB block +' conditions was considered as confirmed. The respective transporter is noted in brackets. PTIP values ≥ 2.5x are highlighted in **bold**.

Compound	Molecular weight (g/mol)	tPSA (Å)	cLogP	LogD _{7.4}	MDCK-LE P _{app} (10 ⁻⁶ cm/s)	K _{p, pred}	K _{p, pred} / MDCK-LE P _{app}	Highest confirmed PTIP
abacavir	286.3	104	1.2	1.2	12.6	16.4	1.30	0.892 (OCT1)
amisulpride	369.5	102	1.3	-0.3	1.6	6.72	4.20	1.61 (OCT1)
atorvastatin	558.7	114	4.4	1.2	3.73	16.7	4.48	2.26 (OATP1B3)
benzbromarone	424.1	50.4	6	3.4	4.2	61.9	14.7	1.51 (OAT3)
bumetanide	364.4	119	3.4	0.03	1.13	8.4	7.43	1.32 (OAT3)
cetirizine	388.9	53	2.1	1.3	4.64	17.8	3.84	1.78 (OCT1)
cimetidine	252.3	88.9	0.3	0.3	1.5	9.63	6.42	1.71 (OCT1)
cyclosporin A	1202.6	279	14.0	4.0	3.71	87.7	23.6	6.78 (OATP1B1)
daclatasvir	738.9	174.6	4.7	4.5	3.72	116	31.2	34.2 (OCT2)
diclofenac	296.2	49.3	4.7	1.2	16.7	16.8	1.01	1.25 (OAT1)
dolutegravir	419.4	101	-0.4	2.1	9.51	28.5	3.00	11.3 (OCT2)
famotidine	337.5	176	-0.6	-0.4	0.87	6.51	7.48	1.73 (MATE2-K)
furosemide	330.7	123	1.9	-1.2	1.1	4.01	3.65	1.44 (OAT1)
gemfibrozil	250.3	46.5	3.9	2.1	12.3	28.5	2.32	1.21 (OAT3)
irinotecan	586.7	116.7	2.7	1.3	1.9	17.5	9.21	5.43 (OCT1)
isavuconazole	437.5	87.6	2.7	3.4	6.17	60.8	9.85	13.2 (OCT2)
ledipasvir	889	175	6.7	> 4.7	0.012	132.6	11050	>255 (OCT1)
ondansetron	293.4	44.8	2.1	1.6	16.9	21.2	1.25	1.57 (MATE1)

DMD # 85993

37

pravastatin	424.5	124	2.0	-0.75	0.56	5.3	9.45	-*
probenecid	285.4	74.7	3.4	-0.7	7.31	5.45	0.75	1.58 (OAT3)
pyrimethamine	248.7	77.8	2.4	2.2	11.7	30.3	2.59	2.09 (MATE2-K)
ranitidine	314.4	86.3	0.7	-0.6	1.3	5.7	4.38	0.668 (MATE1)
ranolazine	427.5	74.3	1.0	0.9	16.8	14.1	0.84	1.35 (OCT1)
rifampicin	823	220	1.5	1.1	1.44	16.3	11.3	1.72 (OATP1B3)
saquinavir	670.9	167	4.7	4.0	2.5	87.7	35.08	4.09 (OCT1)
trimethoprim	290.3	106	0.98	0.6	10.3	11.7	1.14	1.75 (MATE1)
valsartan	435.5	112	4.9	-0.6	0.66	5.78	8.76	1.58 (OAT3)
vandetanib	475.4	59.5	3.7	2.6	8.45	39.4	4.66	4.19 (OCT2)
venetoclax	868.5	174.7	10.0	> 4.7	0.15	132.6	884.0	>258 (OATP1B1)
verapamil	454.6	64	1.5	2.5	14.5	36.1	2.49	3.06 (OCT1)

^a PTIP of pravastatin is missing as IC₅₀ values could not be determined.

Table 2. The preincubation effect of selected inhibitors on OATP1B1, OATP1B3, OAT1, OAT3, OCT1, OCT2, MATE1, and MATE2-K. IC₅₀ was measured after a 3-hour preincubation with vehicle only or inhibitor, and PTIP was calculated as the fold decrease in IC₅₀ caused by preincubation. Experiments were performed using untreated plasticware ('**NSB block -**', N=1) or plasticware pre-coated against nonspecific binding ('**NSB block +**', N=2). In the case of replicate experiments, PTIP was calculated as the ratio of the means of N=2 IC₅₀ values corresponding to vehicle and inhibitor preincubation conditions. For raw IC₅₀ data see **Supplementary Table 4**. PTIP values highlighted in **bold** are equal to or greater than the threshold of 2.5x. N/D, not determined due to weak inhibition.

Inhibitor	PTIP (fold potentiation)			
	NSB block -	NSB block +	NSB block -	NSB block +
	OATP1B1		OATP1B3	
venetoclax	203	>258	>13.2	>8.70
cyclosporin A	5.88	6.78	3.75	3.02
saquinavir	3.17	3.54	4.60	3.78
atorvastatin	1.88		2.26	
rifampicin	1.47		1.72	
gemfibrozil	0.976		0.672	
	OAT1		OAT3	
benzbromarone	1.82		4.96	1.51
furosemide	1.44		0.723	
valsartan	1.40		1.58	
probenecid	1.37		1.58	
diclofenac	1.25		0.428	
bumetanide	1.19		1.32	
gemfibrozil	0.514		1.21	
rifampicin	N/D		N/D	

DMD # 85993

39

saquinavir	N/D		N/D	
pravastatin	N/D		N/D	
	OCT1		OCT2	
ledipasvir	>594	>255	>4.04	>8.73
irinotecan	17.3	5.43	2.12	
saquinavir	7.81	4.09	N/D	
daclatasvir	3.42	5.65	156	34.2
verapamil	3.36	3.06	1.86	
vandetanib	3.14	2.69	5.36	4.19
cetirizine	3.12	1.78	3.35	1.55
isavuconazole	3.00	2.98	5.52	13.2
cimetidine	1.71		N/D	
amisulpride	1.61		1.18	
ranolazine	1.35		1.08	
trimethoprim	1.35		1.28	
abacavir	0.892		N/D	
dolutegravir	N/D		6.20	11.3
	MATE1		MATE2-K	
pyrimethamine	1.88		2.09	
vandetanib	1.81		2.54	3.00
trimethoprim	1.75		1.07	
ondansetron	1.57		1.04	
isavuconazole	1.53		2.46	1.38
cimetidine	1.27		0.747	
famotidine	1.12		1.73	
ranitidine	0.668		0.438	

Table 3. The estimated contribution of toxicity to PTIP. To estimate fold IC₅₀ change caused by the occasional toxicity of a test inhibitor, percent transport values measured without preincubation at each concentration of the compound were multiplied by percent viability values determined after a 3-hour preincubation with the same concentration. Fold IC₅₀ change due to toxicity was either postulated to be 1.0 when the inhibitor did not impair viability by more than 10% even at the highest applied concentration, or estimated as (IC₅₀ without toxicity) / (IC₅₀ with toxicity). Values ≥2.5 are highlighted in **bold**. For more details please refer to the main text and **Supplementary Fig.3**.

Inhibitor	Cell line	A	B	A/B
		Fold IC ₅₀ change due to preincubation (=PTIP)	Fold IC ₅₀ change due to toxicity (<i>estimated or *postulated</i>)	Fold IC ₅₀ change corrected for toxicity (<i>calculated</i>)
cyclosporin A	HEK-OATP1B1	6.78	1.0*	6.78
	HEK-OATP1B3	3.02	1.0*	3.02
daclatasvir	HEK-OCT1	5.65	1.0*	5.65
	HEK-OCT2	34.2	1.0*	34.2
dolutegravir	HEK-OCT2	11.3	1.0*	11.3
irinotecan	HEK-OCT1	5.43	1.0*	5.43
isavuconazole	HEK-OCT1	2.98	1.0*	2.98
	HEK-OCT2	13.2	1.4	9.43
ledipasvir	HEK-OCT1	>255	1.0*	>255
	HEK-OCT2	>8.73	1.0*	>8.73
saquinavir	HEK-OATP1B1	3.54	1.0	3.54
	HEK-OATP1B3	3.78	0.91	4.15
	HEK-OCT1	4.09	1.0*	4.09
vandetanib	HEK-OCT1	2.69	1.4	1.92
	HEK-OCT2	4.19	1.4	2.99

DMD # 85993

41

	MDCKII-MATE2- K	3.00	1.5	2.00
venetoclax	HEK-OATP1B1	>258	1.1	>235
	HEK-OATP1B3	>8.70	4.8	>1.81
verapamil	HEK-OCT1	3.06	1	3.06

Table 4. The effect of preincubation on the outcome of *in vitro* DDI risk assessment.

Maximum steady state total plasma concentration ($C_{max,ss}$) and unbound fraction (f_u) values were taken from the sources referenced below the table. Maximum steady state unbound plasma concentrations ($C_{max,u,ss}$) were calculated as $C_{max,ss} * f_u$, while IC_{50} values are means from N=2 'NSB block +' experiments (see **Supplementary Table X**). Cases when preincubation changed the result of risk prediction are highlighted with grey background on the right.

Inhibitor	$C_{max,ss}$ (μ M)	f_u	Transporter	$C_{max,u,ss}$ /IC ₅₀ -pre	$C_{max,u,ss}$ /IC ₅₀ +pre	Predicted DDI risk w/o preincubation		Predicted DDI risk w/ preincubation		Outcome w/o -> w/ preincubation	
						FDA / PMDA	EMA	FDA / PMDA	EMA	FDA / PMDA	EMA
cyclosporin A ^a	1.83	0.1	OATP1B1	0.2744	1.8626	Y	Y	Y	Y	risk ->	risk -> risk
			OATP1B3	0.3624	1.0958	Y	Y	Y	Y	risk	risk
daclatasvir ^b	2.34	0.01	OCT2	0.0003	0.0118	N	N	N	N	no risk ->	risk? ⁱ ->
			OCT1	0.0439	0.2481	-	Y	-	Y	no risk	risk? ⁱ
dolutegravir ^c	9.9	0.011	OCT2	0.0068	0.0772	N	N	N	Y	no risk ->	no risk ->
isavuconazole ^d	17.1	0.01	OCT2	0.0102	0.1352	N	N	Y	Y	risk ->	risk -> risk
			MATE1	0.0239	0.0366	Y	Y	Y	Y	risk ->	risk -> risk
			MATE2-K	0.0082	0.0114	N	N	N	N	risk	risk
			OCT1	0.0328	0.0980	-	Y	-	Y	risk	risk
irinotecan ^e	2.5	0.32	OCT2	0.0140	0.0296	N	N	N	Y	no risk ->	risk? ⁱ ->
			OCT1	6.6390	35.8744	-	Y	-	Y	no risk	risk
ledipasvir ^f	0.363	<0.01	OCT2	<0.0001	0.0002	N	N	N	N	no risk ->	no risk ->
			OCT1	<0.0001	0.0186	N	N	N	N	no risk	no risk
saquinavir ^e	1.41	0.02	OATP1B1	0.0077	0.0275	N	N	N	Y	no risk ->	no risk ->
			OATP1B3	0.0026	0.0097	N	N	N	N	no risk ->	no risk ->
			OCT1	0.0015	0.0063	-	N	-	N	no risk	risk
vandetanib ^g	3.32	0.06	OCT2	0.0101	0.0422	N	N	N	Y		

DMD # 85993
 43

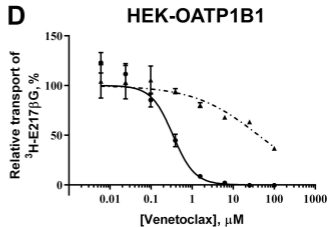
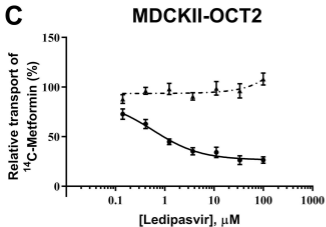
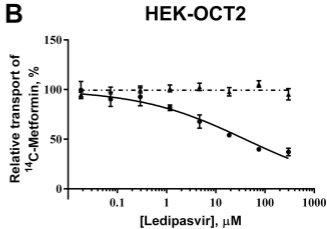
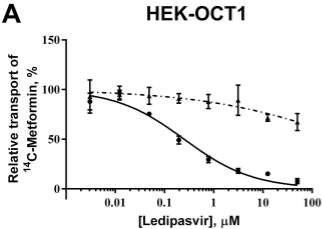
			MATE1	0.2509	0.4548	Y	Y	Y	Y	risk ->	risk? ⁱ ->
			MATE2-K	0.2264	0.6799	Y	Y	Y	Y	risk	risk
			OCT1	0.0382	0.1027	-	Y	-	Y		
venetoclax^h	2.42	<0.01	OATP1B1	0.0006	0.0365	N	N	N	N	no risk ->	no risk ->
			OATP1B3	<0.0001	0.0007	N	N	N	N	no risk	no risk

^a (Vaidyanathan et al., 2016); ^b (FDA, 2015b); ^c (FDA, 2013); ^d (FDA, 2015a); ^e (Goodman et al., 2001); ^f (FDA, 2014); ^g (Tamura et al., 2006); ^h (Emami Riedmaier et al., 2018); ⁱ The outcome of risk assessment depended on the set of assays considered (recommended only: OCT2, or recommended plus optional: OCT2 plus OCT1, MATE1, and MATE2-K).

Table 5. PTIP values and cellular uptake parameters of selected transporter/inhibitor pairs. For comparability across PTIP-positive and PTIP-negative transporter/inhibitor combinations, 'NSB block -' PTIP values are shown in each case. PS_{inf} : cellular uptake clearance normalized to cell number. K_p : ratio of steady state total concentrations measured in the cells vs. medium. When determined in the presence of a specific and potent inhibitor, K_p reflects passive equilibration. $f_{u,cell}$: unbound fraction in the cell. $K_{p,uu}$: ratio of steady state unbound concentrations in the cells vs. medium. $K_{p,uu}$ values >1 indicate active accumulation. For calculations see *Materials and Methods*.

			Cellular uptake parameters					
Transporter	Inhibitor	PTIP (fold)	Time to steady state (min)	PS_{inf}^b ($\mu\text{L}/\text{min}/10^6$ cells)	K_p w/o inhibitor: passive and active	K_p with inhibitor: passive only	$f_{u,cell}$	$K_{p,uu}$
OCT1	ledipasvir	>594	>180 ^a	0.171	155	123	0.00816	1.27
OATP1B1	venetoclax	203	>180 ^a	0.92	266	263	0.0038	1.01
OATP1B1	cyclosporin A	5.88	120	0.92	310	259	0.00387	1.20
OATP1B1	saquinavir	3.17	60	10.4	729	416	0.00256	1.75
OAT3	benzbromarone	4.96	60	8.29	333	333	0.003	1.00
OAT1	benzbromarone	1.82	15	11.1	486	396	0.00253	1.23
OAT3	valsartan	1.40	3	5.59	17.8	1.33	0.752	13.3
OCT2	trimethoprim	1.28	1	9.2	13.3	4.85	0.151	2.73

^a K_p values of ledipasvir and venetoclax were calculated with an approximation assuming steady state was reached at 180 min. ^b Time points used for the calculation of the initial slope: ledipasvir: 1-30 min; venetoclax: 1-90 min; cyclosporine A: 15-120 min; saquinavir: 1-5 min; benzbromarone (OAT1 and OAT3): 1-5 min; valsartan: 0-1 min; trimethoprim: 0-1 min.



▲ w/o preincubation

■ w preincubation

Figure 1

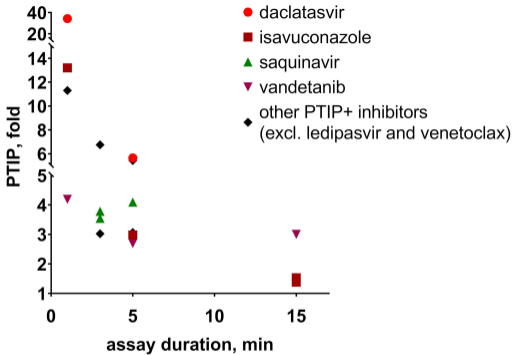


Figure 2

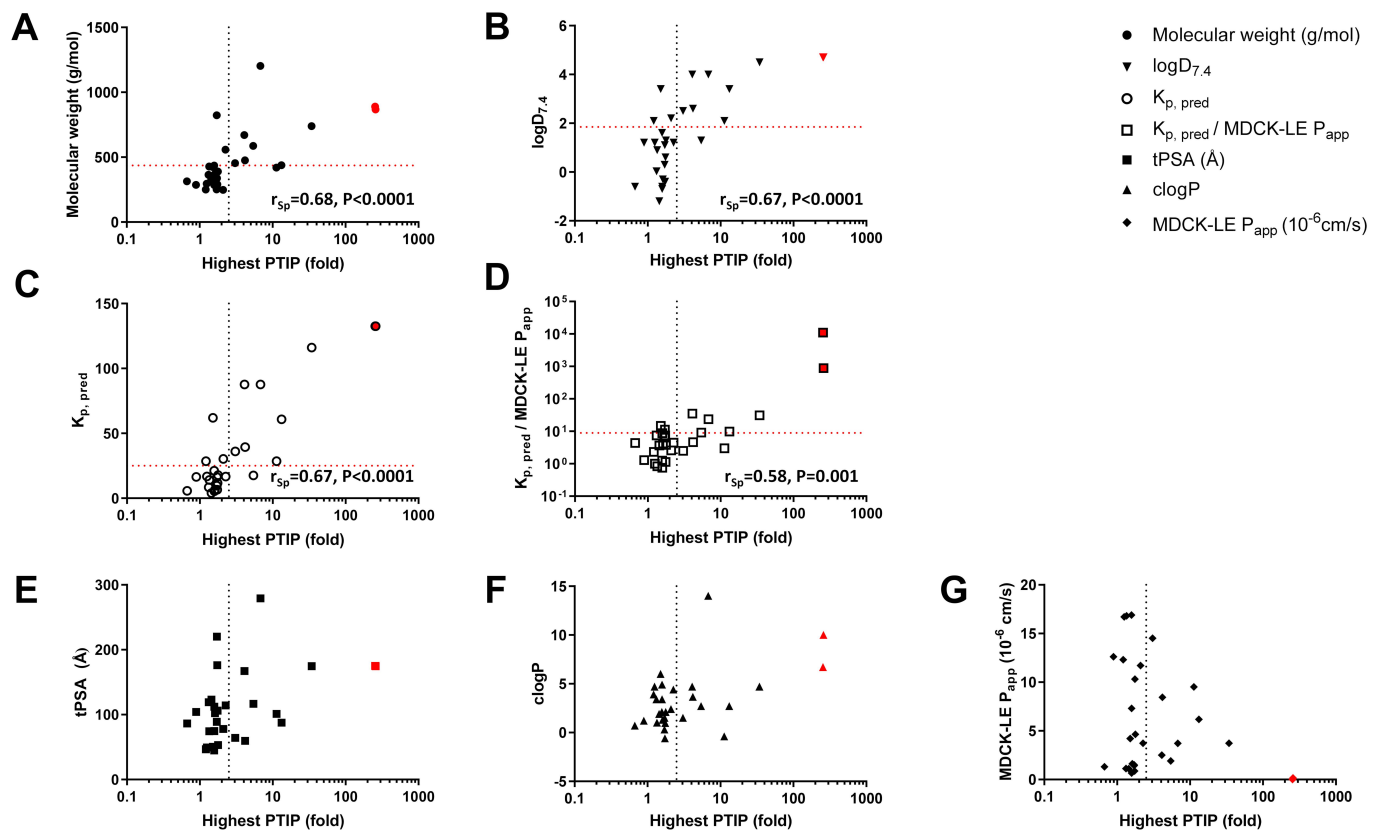


Figure 3

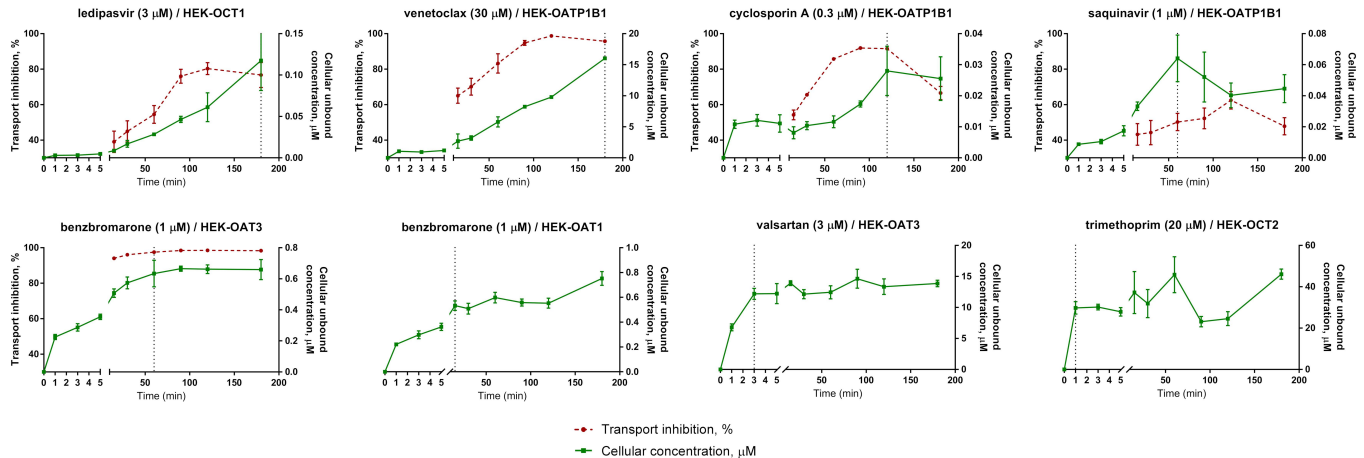
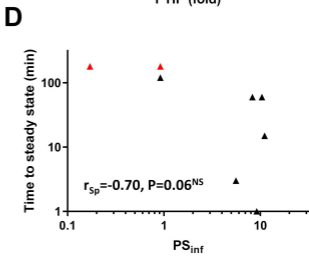
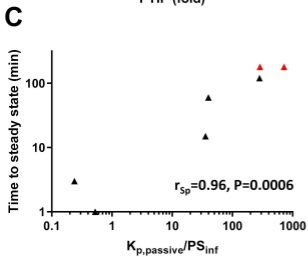
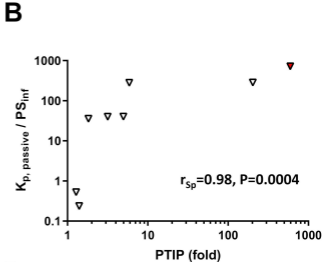
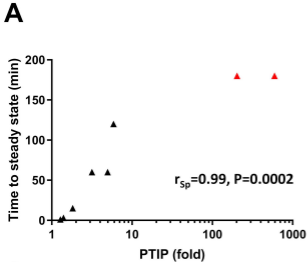


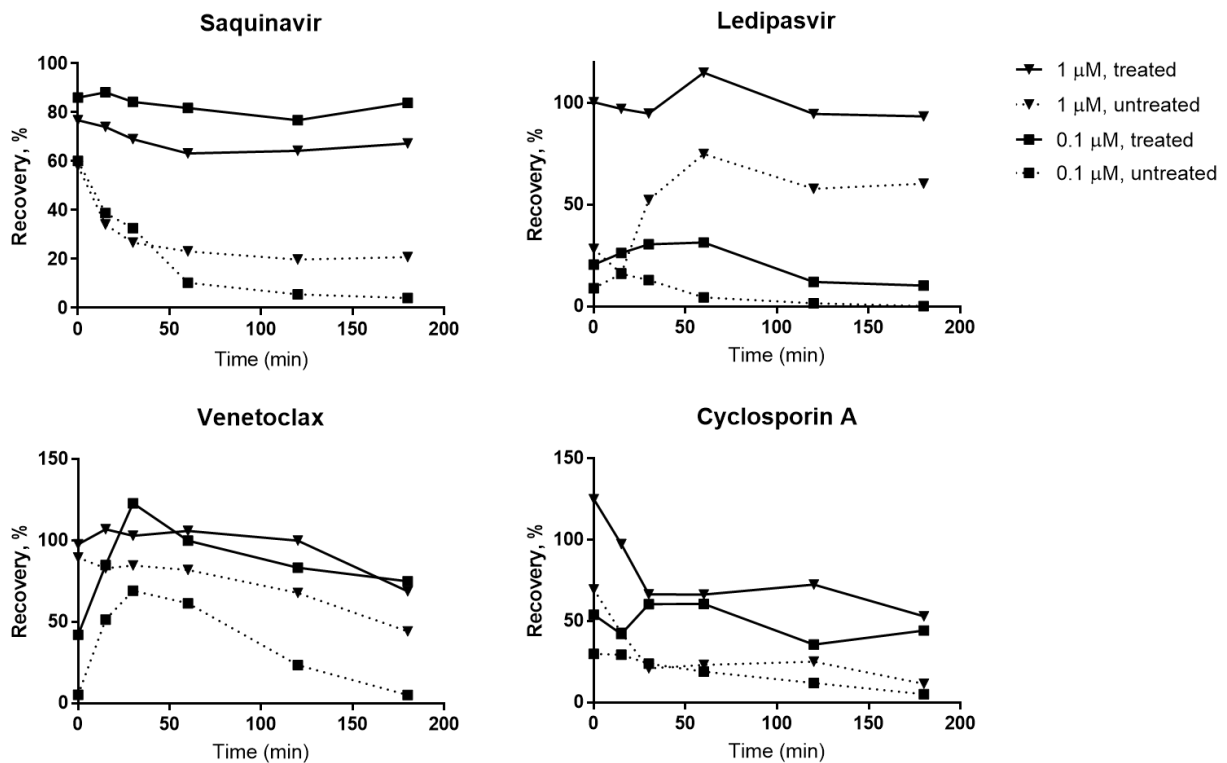
Figure 4



- ▲ Time to steady state (min)
- ▼ $K_{p,passive} / PS_{inf}$

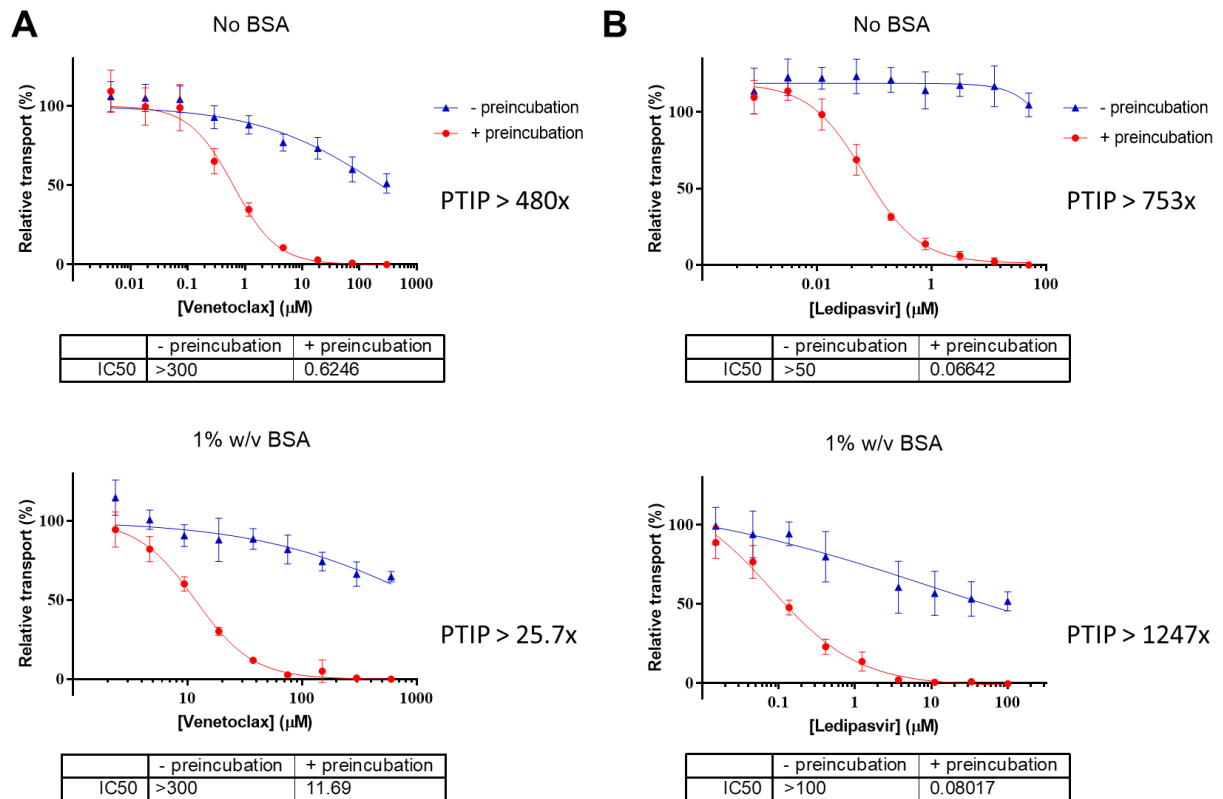
Figure 5

Supplemental Data to Tátrai et al.: A systematic in vitro investigation of the inhibitor preincubation effect on multiple classes of clinically relevant transporters. Drug Metabolism and Disposition.



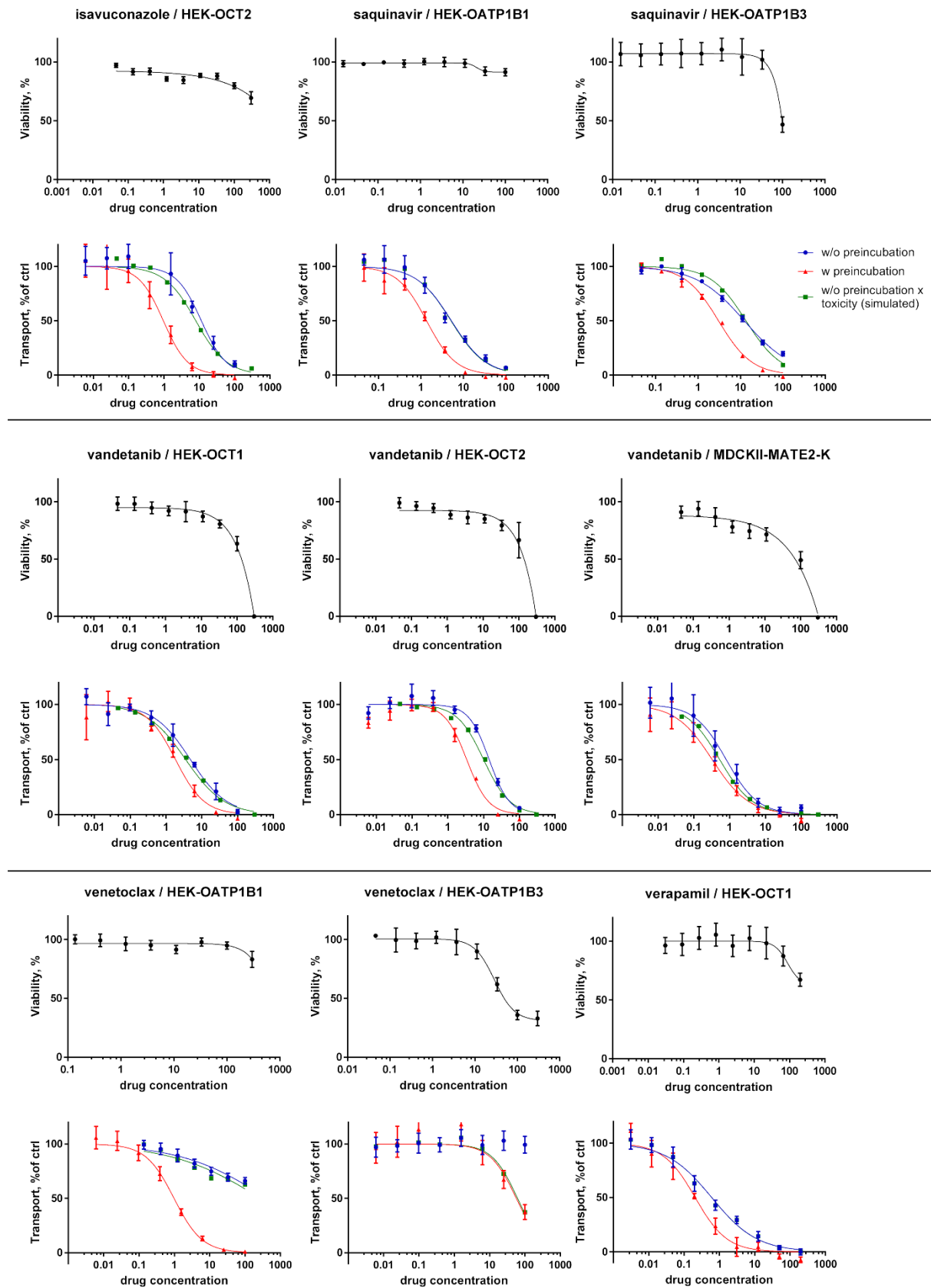
Supplementary Figure 1. The effect of plastic pre-treatment on the recovery of saquinavir, ledipasvir, venetoclax, and CsA. Each compound was incubated in plastic containers that were either untreated or pre-treated with 20% v/v FBS and 2% w/v BSA in HBSS. Percent recovery values of 1 μ M and 0.1 μ M solutions after 15, 30, 60, 120, and 180 min indicate that pre-coating substantially reduces nonspecific binding to plastic.

Supplemental Data to Tátrai et al.: A systematic in vitro investigation of the inhibitor preincubation effect on multiple classes of clinically relevant transporters. Drug Metabolism and Disposition.



Supplementary Figure 2. The preincubation effect persists in the presence of 1% w/v BSA. Although the fold difference in IC₅₀ caused by preincubation was reduced, the addition of BSA did not eliminate the pronounced preincubation effect of venetoclax (**A**) or ledipasvir (**B**). Each point represents the mean \pm SD of N=3 replicates from a single experiment.

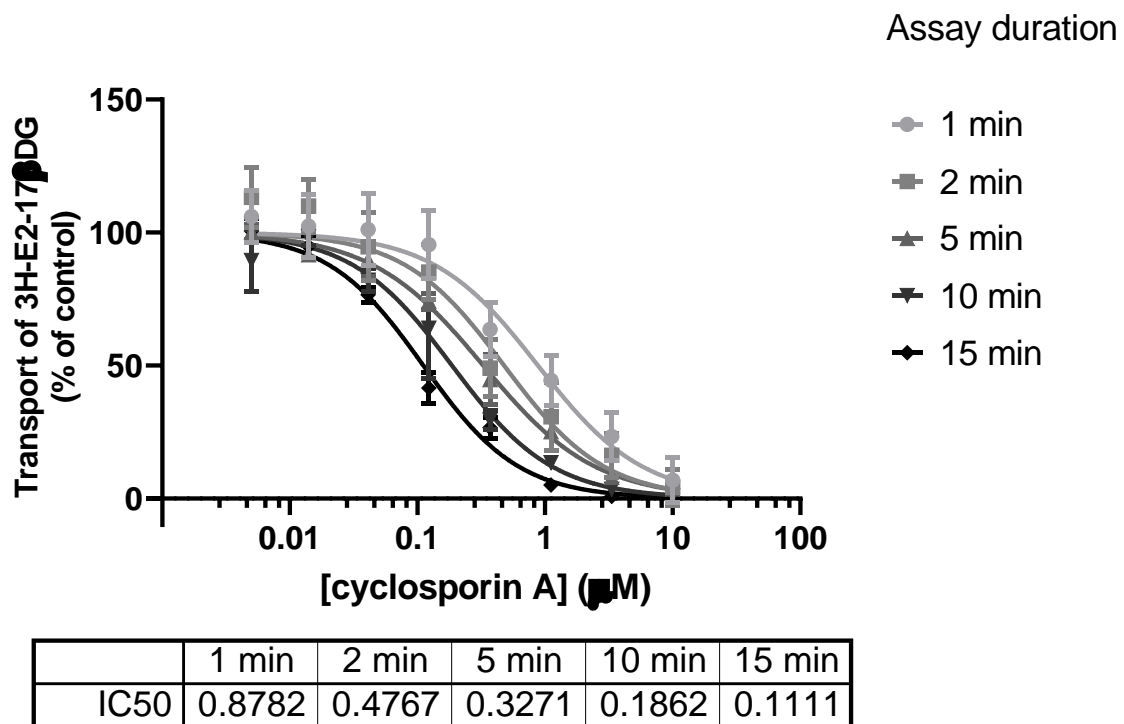
Supplemental Data to Tátrai et al.: A systematic in vitro investigation of the inhibitor preincubation effect on multiple classes of clinically relevant transporters. Drug Metabolism and Disposition.



Supplemental Data to Tátrai et al.: A systematic in vitro investigation of the inhibitor preincubation effect on multiple classes of clinically relevant transporters. Drug Metabolism and Disposition.

Supplementary Figure 3. Estimating the contribution of toxicity to PTIP. For cell line / inhibitor pairs where a 3-hour incubation with a single high concentration of the inhibitor caused $\geq 10\%$ loss of cell viability, LC₅₀ curves were established (upper graphs in each panel with black symbols/line), and percent transport values measured without preincubation (blue symbols) were multiplied by the corresponding percent viability values measured with resazurin assay. The resulting curves (green) represent the estimated effect of toxicity; red symbols/lines show the actual inhibition curves measured with preincubation. Each point represents the mean \pm SD of N=3 replicates from a single experiment. For more explanation see main text and **Table 3**.

Supplemental Data to Tátrai et al.: A systematic in vitro investigation of the inhibitor preincubation effect on multiple classes of clinically relevant transporters. Drug Metabolism and Disposition.



Supplementary Figure 4. The impact of assay duration on IC₅₀ in the absence of preincubation. By increasing coincubation time from 1 min to 15 min, the IC₅₀ of CsA on E2-17βDG transport of OATP1B1 decreased from 0.878 to 0.111. Each measurement point represents N=3 replicates from a single experiment.

Supplemental Data to Tátrai et al.: A systematic in vitro investigation of the inhibitor preincubation effect on multiple classes of clinically relevant transporters. Drug Metabolism and Disposition.

Supplementary Table 1. LC/MS settings used for the quantification of test compounds in media and cell extracts

Compound	Parent mass m/z	Product mass m/z	Polarity	Declustering potential, V	Collision energy, V
abacavir	287.2	191.1	positive	80	25
amisulpride	370.1	241.8	Positive	1	35
atorvastatin	559.3	292.1	positive	60	45
benzbromarone	422.9	276.8	positive	1	35
bumetanide	365.2	240.0	positive	65	25
cetirizine	390.2	202.1	positive	65	25
cimetidine	253.3	95.1	positive	55	35
cyclosporine	602.2	545.4	positive	60	25
daclatasvir	739.4	565.3	positive	100	55
diclofenac	294	250.0	negative	-30	-15
dolutegravir	420.2	277.0	positive	90	35
famotidine	338.3	188.9	positive	50	25
furosemide	330	286.0	negative	-50	-25
gemfibrozil	251.3	223.9	positive	40	25
irinotecan	587.3	502.2	positive	140	45
isavuconazole	438.2	224.0	positive	1	25
ledipasvir	889.5	732.4	positive	1	55
ondansetron	294.2	170.1	positive	1	35
pravastatin	425.4	207.0	positive	70	35
probenecid	284.1	240.0	negative	-55	-25
pyrimethamine	249.4	177.1	positive	1	45
ranitidine	315.2	176.1	positive	100	25
ranolazine	428.3	98	positive	25	50
rifampicin	821.2	397.3	negative	-190	-55
saquinavir	671.1	570.3	positive	1	45
trimethoprim	291	230.1	positive	40	40
valsartan	463.3	235.1	positive	50	25
vandetanib	475.1	111.9	positive	70	15
venetoclax	868.3	321.1	positive	1	45
verapamil	455.5	165.0	positive	90	35

Supplemental Data to Tátrai et al.: A systematic in vitro investigation of the inhibitor preincubation effect on multiple classes of clinically relevant transporters. Drug Metabolism and Disposition.

Supplementary Table 2. Reagents and conditions used in uptake inhibition assays

Transporter	Substrate	Radiolabeled tracer ^a	Total substrate conc. in the assay (μM)	Radioactive conc. of tracer in the assay (μCi/mL)	Assay buffer ^b	Assay duration (min)	Reference inhibitor (μM)
OATP1B1	β-Estradiol 17-(β-D-glucuronide)	PerkinElmer NET1106250UC (³ H)	1	2	HBSS	3	rifampicin (50)
OATP1B3			1	2	HBSS	3	rifampicin (50)
OAT1	p-Aminohippuric acid	PerkinElmer NET053001MC (³ H)	5	2	HBSS	2	benzbromarone (300)
OAT3	Estrone 3-sulfate	BRC Radiolab BL-104 (³ H)	1	2	HBSS	1	probenecid (500)
OCT1	Metformin	Moravek MC2043 (¹⁴ C)	10	0.4	HBSS	5	verapamil (200)
OCT2			10	0.4	HBSS	1	verapamil (200)
MATE1			10	0.2	KH	15	pyrimethamine (1)
MATE2-K			10	0.2	KH	15	pyrimethamine (10)

^a PerkinElmer, Waltham, MA; BRC Radiolab: Radiochemistry Lab of the Biological Research Center, Szeged, Hungary; Moravek, Brea, CA

^b HBSS: Hanks' Balanced Salt Solution, pH 7.4 (ThermoFisher, Waltham, MA); KH: Krebs-Henseleit buffer (23.8 mM NaHCO₃, 4.8 mM KCl, 0.96 mM K₂HPO₄, 1.2 mM MgSO₄, 12.6 mM HEPES, 5 mM glucose, 1.5 mM CaCl₂, 142 mM NaCl), pH 8.0

Supplemental Data to Tátrai et al.: A systematic in vitro investigation of the inhibitor preincubation effect on multiple classes of clinically relevant transporters. Drug Metabolism and Disposition.

Supplementary Table 3. Health authority guideline recommendations on transporter-based DDI risk assessment *in vitro*. $I_{inlet,max,u}$: maximum unbound plasma concentration at the liver inlet, calculated as $f_u * (C_{max} + F_a F_g * k_a * Dose / Q_h * R_B)$, where f_u is the unbound fraction, C_{max} is maximum plasma concentration, F_a is the fraction absorbed, F_g is the intestinal availability, k_a is the absorption rate constant, Q_h is the hepatic flow rate (taken to be 1450 mL/min), and R_B is the blood-to-plasma concentration ratio (taken to be 1). If unknown, $F_a F_g = 1$ and $k_a = 0.1/\text{min}$ are used. The unbound fraction f_u should be set to 0.01 if the experimentally determined value is lower.

	FDA and PMDA		EMA	
	Recommendation	Risk calculation	Recommendation	Risk calculation
OATP1B1/3	recommended	$I_{inlet,max,u}/IC_{50} \geq 0.1$	recommended	$I_{inlet,max,u}/IC_{50} \geq 0.04$
OAT1/3, OCT2	recommended	$I_{max,u}/IC_{50} \geq 0.1$	recommended	$I_{max,u}/IC_{50} \geq 0.02$
MATE1/2-K	recommended	$I_{max,u}/IC_{50} \geq 0.02$	to be considered	$I_{max,u}/IC_{50} \geq 0.02$
OCT1	no recommendation	-	to be considered	$I_{inlet,max,u}/IC_{50} \geq 0.04$

Supplemental Data to Tátrai et al.: A systematic in vitro investigation of the inhibitor preincubation effect on multiple classes of clinically relevant transporters. Drug Metabolism and Disposition.

Supplementary Table 4. The preincubation effect of selected inhibitors on OATP1B1, OATP1B3, OAT1, OAT3, OCT1, OCT2, MATE1, and MATE2-K: extended data. The table shows the effect of a 3-hour preincubation on IC₅₀, where '-pre' indicates IC₅₀ without preincubation (vehicle control), '+pre' indicates IC₅₀ with inhibitor preincubation, and PTIP is the fold decrease in IC₅₀ caused by preincubation. Initial IC₅₀ measurements with untreated auxiliary plates ('NSB block -') were performed once. Confirmatory measurements with pre-coated plates ('NSB block +') were done twice, and PTIP was calculated from the means of N=2 IC₅₀ values. Mean IC₅₀ values and PTIP calculated from means are shown in *italic*. PTIP ≥ 2.5 is highlighted in **bold**. N/D, not determined due to weak or no inhibition.

Inhibitor	NSB block -			NSB block +			NSB block -			NSB block +		
	IC ₅₀ , μM		PTIP	IC ₅₀ , μM		PTIP	IC ₅₀ , μM		PTIP	IC ₅₀ , μM		PTIP
	-pre	+pre		-pre	+pre		-pre	+pre		-pre	+pre	
	OATP1B1						OATP1B3					
venetoclax				>300	0.983					>300	57.2	
				41.3	0.342					>300	11.8	
	231	1.14	203	>171	0.663	>258	>300	22.7	>13.2	>300	34.5	>8.70
cyclosporin A				0.799	0.112					0.360	0.118	
				0.535	0.0845					0.650	0.216	
	0.717	0.122	5.88	0.667	0.0983	6.78	0.612	0.163	3.75	0.505	0.167	3.02
saquinavir				5.22	1.35					12.3	3.02	
				2.08	0.703					9.79	2.79	
	3.23	1.02	3.17	3.65	1.03	3.54	7.86	1.71	4.60	11.0	2.91	3.78
atorvastatin	1.68	0.892	1.88				0.710	0.314	2.26			
rifampicin	1.20	0.818	1.47				3.67	2.13	1.72			
gemfibrozil	32.9	33.7	0.976				246	366	0.672			
	OAT1						OAT3					
benzbromarone										6.20	3.25	
										5.31	4.39	
	2.68	1.47	1.82				1.37	0.276	4.96	5.76	3.82	1.51
furosemide	45.5	31.7	1.44				5.98	8.28	0.723			
valsartan	22.7	16.2	1.40				3.57	2.26	1.58			
probenecid	14.4	10.5	1.37				3.01	1.91	1.58			
diclofenac	8.64	6.89	1.25				3.10	7.24	0.428			
bumetanide	50.8	42.6	1.19				3.35	2.53	1.32			
gemfibrozil	12.7	24.7	0.514				7.46	6.14	1.21			
rifampicin	>100	>100	N/D				>100	>100	N/D			
saquinavir	>100	>100	N/D				>100	>100	N/D			
pravastatin	>300	>300	N/D				>300	>300	N/D			

Supplemental Data to Tátrai et al.: A systematic in vitro investigation of the inhibitor preincubation effect on multiple classes of clinically relevant transporters. Drug Metabolism and Disposition.

	OCT1						OCT2					
ledipasvir				>50	0.251					>300	39.0	
				>50	0.140					>100	6.75	
	>300	0.505	>594	>50	0.196	>255	>300	74.3	>4.04	>200	22.9	>8.73
irinotecan				0.104	0.0191							
				0.137	0.0255							
	1.24	0.0717	17.3	0.121	0.0223	5.43	57.3	27.0	2.12			
saquinavir				22.6	6.58							
				13.8	2.31							
	78.1	10.00	7.81	18.2	4.45	4.09	>100	>100	N/D			
daclatasvir				0.533	0.120					89.7	2.26	
				0.532	0.0686					45.9	1.69	
	0.574	0.168	3.42	0.533	0.0943	5.65	215	1.38	156	67.8	1.98	34.2
verapamil				0.608	0.207							
				0.310	0.0938							
	1.70	0.505	3.36	0.459	0.150	3.06	36.2	19.5	1.86			
vandetanib				4.80	1.84					14.3	3.37	
				5.64	2.04					25.3	6.07	
	7.86	2.50	3.14	5.22	1.94	2.69	27.9	5.21	5.36	19.8	4.72	4.19
cetirizine				101	49.7					91.0	57.2	
				81.9	52.8					134	88.9	
	101	32.4	3.12	91.5	51.3	1.78	191	57.0	3.35	113	73.1	1.55
isavuconazole				6.20	1.97					11.4	0.960	
				4.22	1.52					22.1	1.57	
	6.07	2.02	3.00	5.21	1.75	2.98	6.29	1.14	5.52	16.8	1.27	13.2
cimetidine	150	87.6	1.71				>300	>300	N/D			
amisulpride	25.3	15.7	1.61				150	127	1.18			
ranolazine	66.9	49.5	1.35				235	218	1.08			
trimethoprim	27.8	20.6	1.35				98.3	77.0	1.28			
abacavir	99.9	112	0.892				>300	>300	N/D			
dolutegravir										27.0	2.43	
										4.81	0.390	
	>300	>300	N/D				23.0	3.71	6.20	15.9	1.41	11.3
	MATE1						MATE2-K					
pyrimethamine	0.03614	0.01927	1.88				0.106	0.0507	2.09			
vandetanib										0.800	0.324	
										0.960	0.262	
	0.794	0.438	1.81				0.875	0.344	2.54	0.880	0.293	3.00
trimethoprim	14.1	8.05	1.75				1.13	1.06	1.07			
ondansetron	0.0913	0.0580	1.57				0.354	0.342	1.04			
isavuconazole										17.0	12.2	
										24.6	17.9	
	7.16	4.67	1.53				41.1	16.7	2.46	20.8	15.1	1.38
cimetidine	4.32	3.41	1.27				7.54	10.1	0.747			
famotidine	1.63	1.45	1.12				54.1	31.2	1.73			

Supplemental Data to Tátrai et al.: A systematic in vitro investigation of the inhibitor preincubation effect on multiple classes of clinically relevant transporters. Drug Metabolism and Disposition.

ranitidine	13.1	19.6	0.668	18.8	42.9	0.438
-------------------	------	------	-------	------	------	-------

Supplemental Data to Tátrai et al.: A systematic in vitro investigation of the inhibitor preincubation effect on multiple classes of clinically relevant transporters. Drug Metabolism and Disposition.

Supplementary Table 5. Single-point toxicity assessment of PTIP-positive inhibitors.

Cell cultures were incubated with each compound at the indicated concentration for 3 hours, and cell viability was determined using CellTiter-Glo™ ATP quantification. Results showing toxicity $\geq 10\%$ are highlighted in **bold**.

Inhibitor	Cell line	Conc. (μM)	Viability (% of control)
cyclosporin A	HEK-OATP1B1	10	96.6 \pm 4.8
	HEK-OATP1B3	10	102.2 \pm 3.6
daclatasvir	HEK-OCT1	50	106.3 \pm 6.5
	HEK-OCT2	50	96.2 \pm 4.6
dolutegravir	HEK-OCT2	300	103.2 \pm 4.3
irinotecan	HEK-OCT1	50	102.8 \pm 3.3
isavuconazole	HEK-OCT1	300	95.0 \pm 6.7
	HEK-OCT2	300	32.2 \pm 2.8
ledipasvir	HEK-OCT1	300	110.2 \pm 8.3
	HEK-OCT2	300	111.1 \pm 7.3
saquinavir	HEK-OATP1B1	100	55.2 \pm 11.9
	HEK-OATP1B3	100	64.3 \pm 6.3
	HEK-OCT1	100	96.5 \pm 7.8
vandetanib	HEK-OCT1	300	0.1 \pm 0.1
	HEK-OCT2	300	0.2 \pm 0.1
	MDCKII-MATE2-K	300	0.4 \pm 0.1
venetoclax	HEK-OATP1B1	100	89.6 \pm 4.1
	HEK-OATP1B3	100	60.2 \pm 4.1
verapamil	HEK-OCT1	100	88.7 \pm 5.8

Supplemental Data to Tátrai et al.: A systematic in vitro investigation of the inhibitor preincubation effect on multiple classes of clinically relevant transporters. Drug Metabolism and Disposition.

Supplementary Table 6. Matrix showing correlations between the physicochemical properties of test compounds. Spearman's rho (r_{sp}) correlation coefficients were calculated for the physicochemical properties listed in **Table 1**. Asterisks indicate the level of significance; ns, not significant.

Nonparametric correlations (r_{sp})	MW (g/mol)	PSA (Å)	cLogP	LogD _{7.4}	MDCK-LE P _{app} (10 ⁻⁶ cm/s)	K _{p, pred}	K _{p, pred} / MDCK-LE P _{app}
MW (g/mol)		0.56**	0.50**	0.55**	-0.40*	0.55**	0.74***
PSA (Å)	0.56**		0.14 ^{ns}	0.05 ^{ns}	-0.72***	0.04 ^{ns}	0.66***
cLogP	0.50**	0.14 ^{ns}		0.56**	-0.19 ^{ns}	0.57**	0.50**
LogD _{7.4}	0.55**	0.05 ^{ns}	0.56**		0.14 ^{ns}	1.00***	0.50**
MDCK-LE P _{app} (10 ⁻⁶ cm/s)	-0.40*	-0.72***	-0.19 ^{ns}	0.14 ^{ns}		0.14 ^{ns}	-0.72***
K _{p, pred}	0.55**	0.04 ^{ns}	0.57**	1.00***	0.14 ^{ns}		0.49**
K _{p, pred} / MDCK-LE P _{app}	0.74***	0.66***	0.50**	0.50**	-0.72***	0.49**	